MSC THESIS SUPPLAMENTARY DOCUMENT

Hydro-Archeological Modeling of Neo-Assyrian Watercourses: Methodology

Student: Alexis Stampoultzidis
Student Number: 4799933

Table of Contents

Archeological Canal data *5*

  Local Systems *6*

  Regional System *8*

  Irrigable fields per canal *10*

Climate-Soil *11*

Crop Growth Simulation *12*

  Assyrian Barley *13*

  Irrigated Area to Harvest and Water Demand *14*

  AquaCrop *14*

Sobek *22*

  Canal Adaptations in Sobek *23*

  Detailed Canal Descriptions *26*

  Control Scenarios *35*

  Input Scenarios *36*

  Calibration-Model Runs *41*

References *43*

Lists of Figures and Tables

Figures

Figure 1Sennacherib's four canal stages with dashed white-black line indicating the LoNAP study area, a map provided by the LoNAP team. 5
Figure 2 Local and Regional System canals routes, along with the excluded Taribisu. 6
Figure 3 Cross-sections used in reconstructing Faida, data acquired from LoNAP team. 7
Figure 4 Bed slope data from LoNAP team, with slopes ranging from 0,5 to 0,7 m/Km in reaches containing offtakes. 8
Figure 5 An example part of the Faida canal exhibiting a rectangular cross-section, by the LoNAP team. 8
Figure 6 More detailed look on Faida, Maltai, Khinis, Bandawai, Uskof and Ba'dreh canals, provided by the LoNAP team. 9
Figure 7 Trial trench 834 cross-section shape indicated by red line (Morandi Bonacossi, 2019). 10
Figure 8 Trial trench cross-section 133 (Morandi Bonacossi, 2019). 10
Figure 9 Jerwan Aqueduct trial trench 900 cross-section, by LoNAP team. 10
Figure 10 Irrigable land of both Regional and Local systems, with orange dots indicating identified offtakes and red the additional ones. 12
Figure 11 AquaCrop main menu, FAO software. 15
Figure 12 Climate parameter inputs AquaCrop. 16
Figure 13 Left screen presenting Harvest index, while right screen crop water productivity. 17
Figure 14 Irrigation schedule menu, as provided by AquaCrop. 18
Figure 15 Total available water TAW, hydraulic conductivity for the left Navkur-Faida soil and right Nineveh’s soil. 19
Figure 16 The Regional canal system is shown in the left while the Local on the right, green dots that are hollow represent canal origins or outputs (offtakes) while full green dots junctions between canals. 23
Figure 17 Faida canal 3,3 m width and 0.5 m water depth cross-section. 25
Figure 18 Faida canal 3,8 m width and 0.5 m water depth cross-section. 25
Figure 19 Faida canal 4,2 m width and 0.5 m water depth cross-section. 25
Figure 20 Khinis cross-section 133 6 m width and 1,6 m water depth. 26
Figure 21 Khinis cross-section 834 4,8 m width and 1,6 m water depth. 26
Figure 22 Jerwan aqueduct cross-section 14,5 m width and 2,5 m water depth. 26
Figure 23 Faida canal cross-section placement. 27
Figure 24 Maltai canal cross-section and roughness placement. 28
Figure 25 Bandawai tunnel cross-section on the left with the tunnel shape on the right, with 0.6 m width, 0.8 m height. 28
Figure 26 Bandawai upper section showing the extent of the tunnel cross-section and the beginning of the 4,8 X 1,6 m. 29
Figure 27 Bandawai cross-section used for earthen reaches emulating Khinis 834 cross-section. 29
Figure 28 Bandawai thin strip and Bandawai mid sections. 30
Figure 29 Bandawai River cross-section estimation based on the Jerwan aqueduct. 30
Figure 30 Uskof upper and lower thin strips, where the beginning of the canalized section is shown. 31
Figure 31 Khinis 133 cross-section adaptation is Sobek. 31

Figure 32 Khinis 834 cross-section adaptation in Sobek. 32
Figure 33 Khinis upper section, marking the start of each cross-section. 32
Figure 34 Jerwan aqueduct Sobek adaptation. 33
Figure 35 Jerwan area with the aqueduct's extents shown. 33
Figure 36 Badreh canals along with Khosr tributary. 34
Figure 37 Khosr canalized river and Kissiri earthen route. 34
Figure 38 Offtake with a 2 m width and 1 m water depth. 35
Figure 39 Local system, Maltai and Faida's input locations are shown in red while streams/wadis in green, along with archeologically identified settlements. 38
Figure 40 Bandawai-Uskof canals, nearby settlements, streams crossing them (green) and input locations (red). 39
Figure 41 Khosr and Kissiri reaches with nearby settlements, streams crossing them (green) and input locations (red). 39
Figure 42 Khinis, Jerwan, Badreh and Khosr tributary reaches with nearby settlements, streams crossing them (green) and input locations (red). 40
Figure 43 Drainage basins associated with canals (pink) and their area in hectares, along with rivers, streams/wadis (green) and bigger settlements in the area. 41

Tables

Table 1 Identified and added offtakes per area. 10
Table 2 Coordinates used for precipitation and temperature data. 12
Table 3 Dry harvest yield for Rainfed, Net water requirement and 20-30-40 mm delivery schedules during Spring-Autumn seasons and Wet-Dry years. 18
Table 4 Maximum days to complete an irrigation event along with total amounts in (mm/ha) and number of events per year and season. 19
Table 5 Dry year 30 mm delivery amount irrigation schedule, presenting available days to irrigate for each event and its fraction to multiply with coverage percentage. 20
Table 6 Wet year 30 mm delivery amount irrigation schedule, presenting available days to irrigate for each event and its fraction to multiply with coverage percentage. 21
Table 7 Canal slopes and archeologically identified cross-sections. 23
Table 8 Canal bed material types and their Manning roughness used in Sobek. 24
Table 9 Offtakes deemed necessary to irrigate, offtake number added and each canal's irrigable land in hectares, followed by required flow (m3/s) per offtake and area in the available days (Wet season). The last two rows show summaries for the Region and Local systems. 26
Table 10 Weirs used, and gates manipulated per canal reach, Heavy and Limited Control scenarios for both 1 and 2 m offtake width scenarios. Their sums are provided at the two bottom rows. 36
Table 11 Canal with associated drainage basin area in hectares, required delivery flow, estimated annual mean, cool season flow, as well as Min and Max cool season inflow. 37
Table 12 1 m Offtake width input flows m3/s per area, Control, and Input scenarios. 42
Table 13 2 m Offtake width input flows m3/s per area, Control and Input scenario. 43

Methodology

In this section, a thorough documentation of methods used for scenario building will be presented. The overview consists of four parts:

1. **Archeological data on canals** and their **delineated irrigable** l**ands**
2. **Climate-Soil** characteristics
3. Crop modelling assumptions through **AquaCrop** for harvest estimations; and lastly
4. Determining scenarios in **Sobek** the numerical model used for flow simulations.

Archeological Canal data

Canals reconstructed in this thesis include most of the infrastructure attributed to Sennacherib, from stages 1, 3 and 4. The second stage Musri canals are excluded due to lack of clear estimations for their routes and other properties like slopes, offtakes, and bed material. Stages 3 and 4 fall entirely within LoNAP's (Land of Nineveh Archeological Project) study area. The Tarbisu canal, which lies just north-west of Nineveh, is excluded as it shows different properties compared to other Neo-Assyrian canals regarding following natural contours, having inconsistent widths for both cross-watershed and more irrigation-oriented canals, and consisting of smaller spoil banks than expected (Ur, 2005).

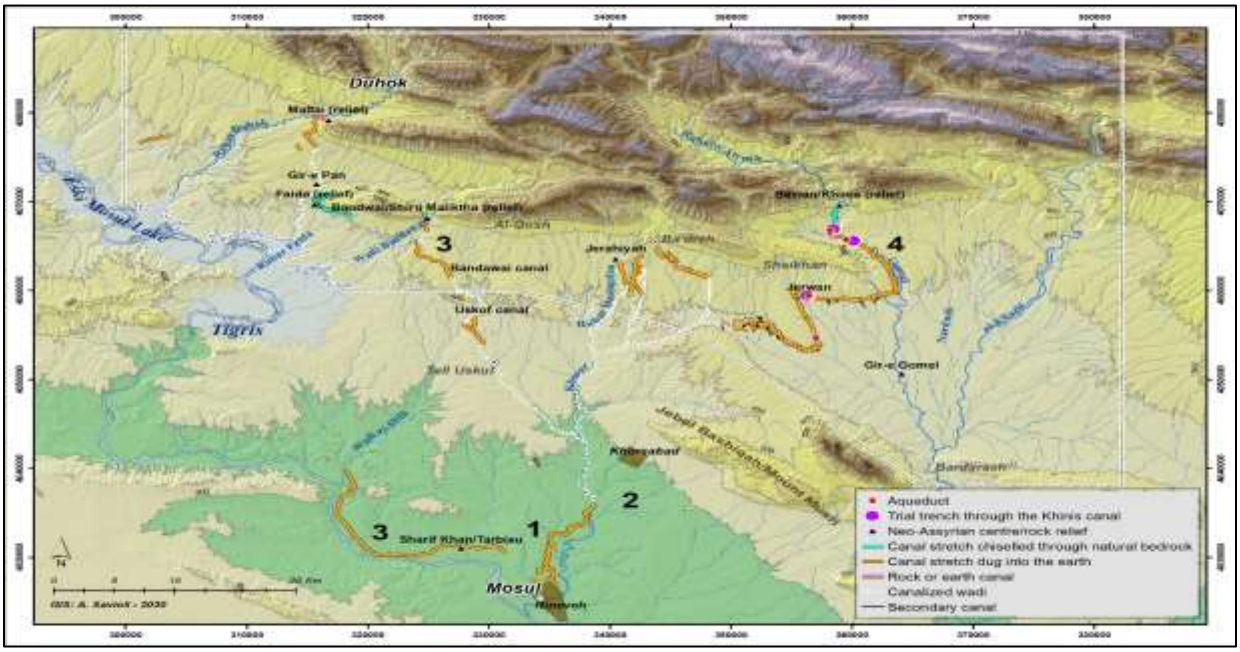

Figure 1Sennacherib's four canal stages with dashed white-black line indicating the LoNAP study area, a map provided by the LoNAP team.

Data on slopes, canal routes, bed material and cross-sections are courtesy of the LoNAP Team, especially Daniele Morandi Bonacossi and Alberto Savioli and the Italian Archeological Mission to the Kurdistan Region of Iraq. For canals not situated within the LoNAP study area boundaries, or in the absence of field data (especially regarding bed slopes), Jason Ur's (Ur, 2005) satellite imagery estimations are used, as early field work done for Khinis and Faida roughly validate his estimations (Morandi Bonacossi, 2019).

The total set of canals is divided into two sets of canals systems: **Local** (Maltai and Faida) and **Regional** (Khinis, Ba'dreh, Bandawai, Uskof and Kisiri). This division stresses their probable (primary) roles, with the former focusing on local irrigation needs (given that they are not connected to other water features), and the latter possibly both aiming to convey water towards the capital and simultaneously irrigating fields along its route (but to an unknown extent).

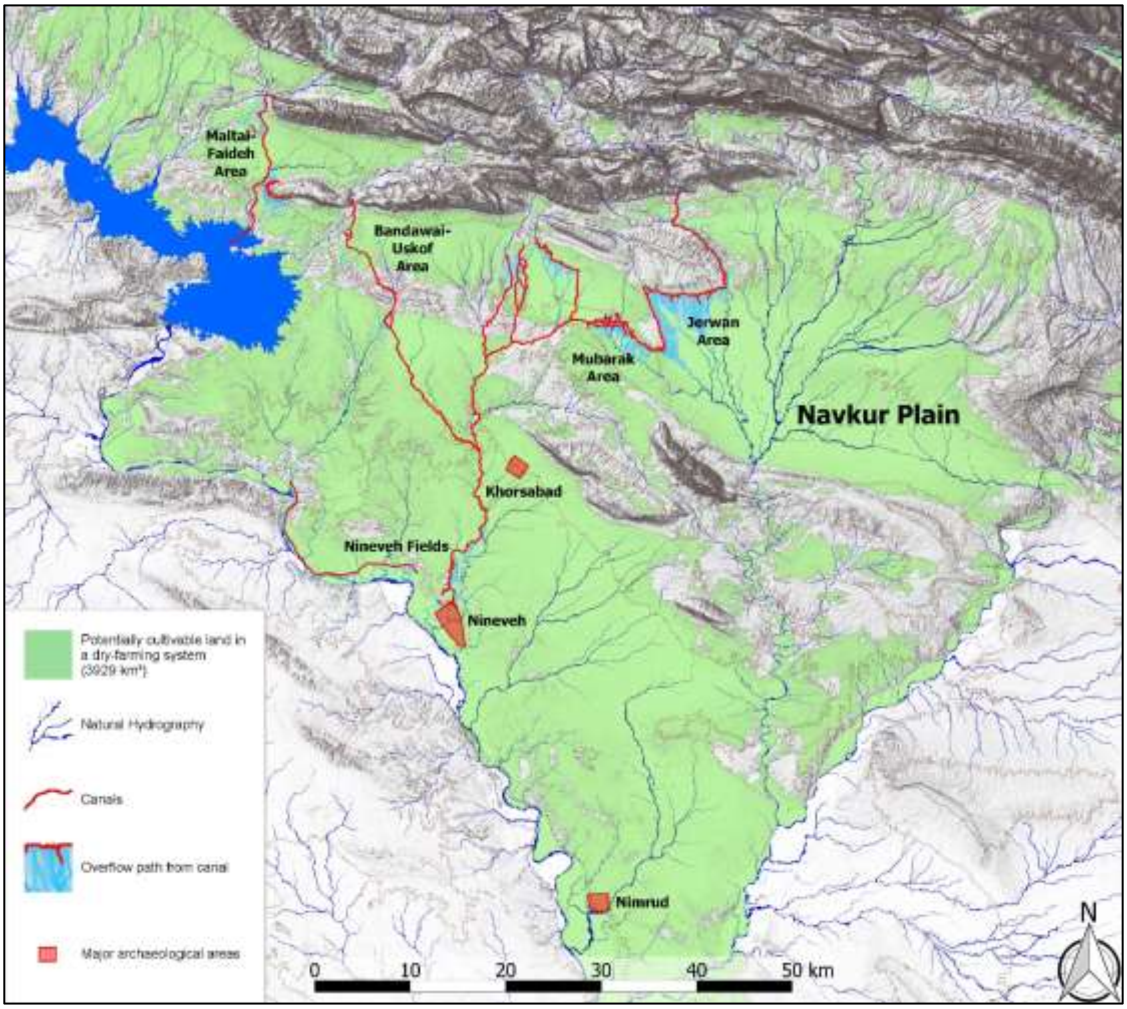

Figure 2 Local and Regional System canals routes, along with the excluded Taribisu.

Local Systems

Maltai is described as a cross-watershed canal, connecting the basins of Rubar Dohuk and Rubar Faida, potentially irrigating fields along the way. Its spoil banks are roughly 80 m wide, an indication of large-scale earthwork, while it is fed at its origin from the river Dohuk through a dam or by withdrawing water from about 2 Km upstream (potentially both). Field data do not exist for this canal and a satellite-derived general slope of 4 m per Km is assumed, while cross sections similar to Faida (see below) are used. The bed material is characterized as “earthwork” until the Gir-e Pan settlement and as “canalized river” for the rest.

Faida is a spring-fed canal on the West side of the Jebel Al-Qosh hill. The canal has 4 offtakes identified (when canal was defined, now 11 have been added) and field estimates for cross-sections, bed slopes and bed material (natural bed rock). According to information provided by the LoNAP team in the figure below, cross sections 219-220 have a 4,20 m bottom width, 216 has 3,8 m and 68 has 3,30 m. All cross-section shapes are considered rectangular in the main route, as there are sculpted Assyrian reliefs found around 0,5 m height from the canal bed, indicating an intended maximum water depth. For this canal, a more detailed data set for bed slope was available, shown in Figure 4. Figure 5 presents a part of the Faida canal showing a rather rectangular-shaped cross-section.

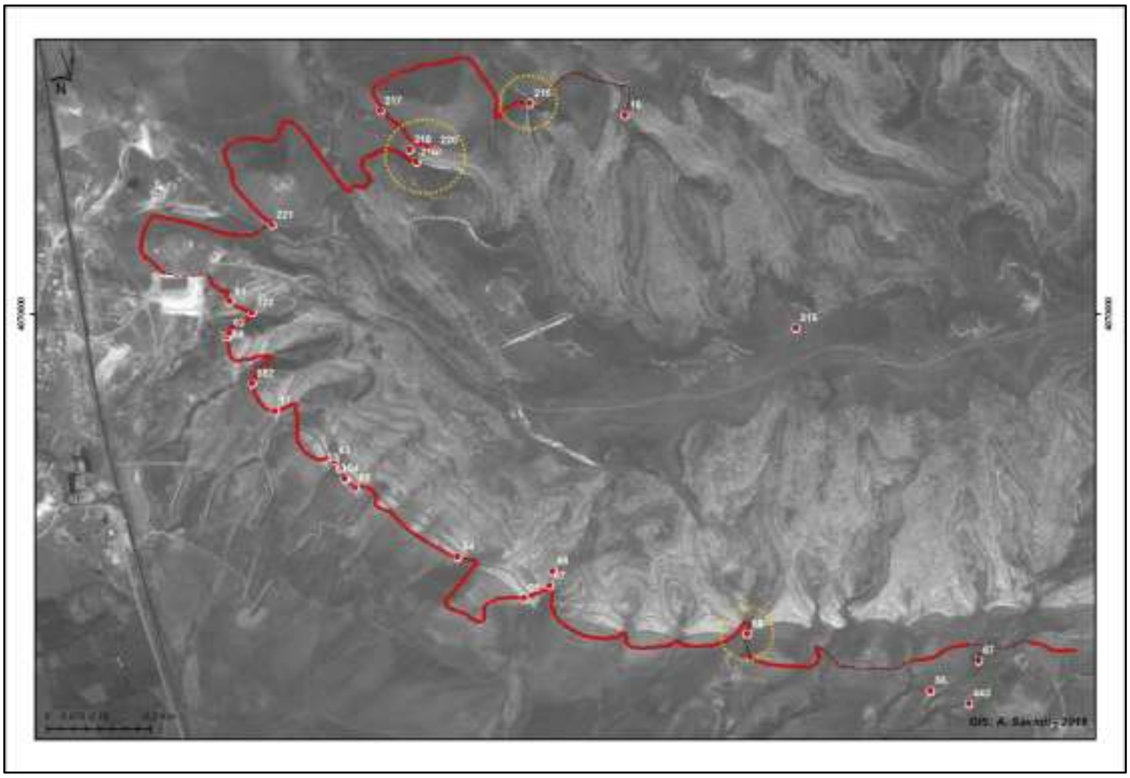

Figure 3 Cross-sections used in reconstructing Faida, data acquired from LoNAP team.

Figure 4 Bed slope data from LoNAP team, with slopes ranging from 0,5 to 0,7 m/Km in reaches containing offtakes.

Figure 5 An example part of the Faida canal exhibiting a rectangular cross-section, by the LoNAP team.

Regional System

Khinis stretches 55 Km from the homonym village, passing above the Navkur plain before meeting the Khosr tributary. The Jerwan aqueduct is indicated below in Figure 6, along with the other two cross-sections 834 and 133, identified by the purple dots.

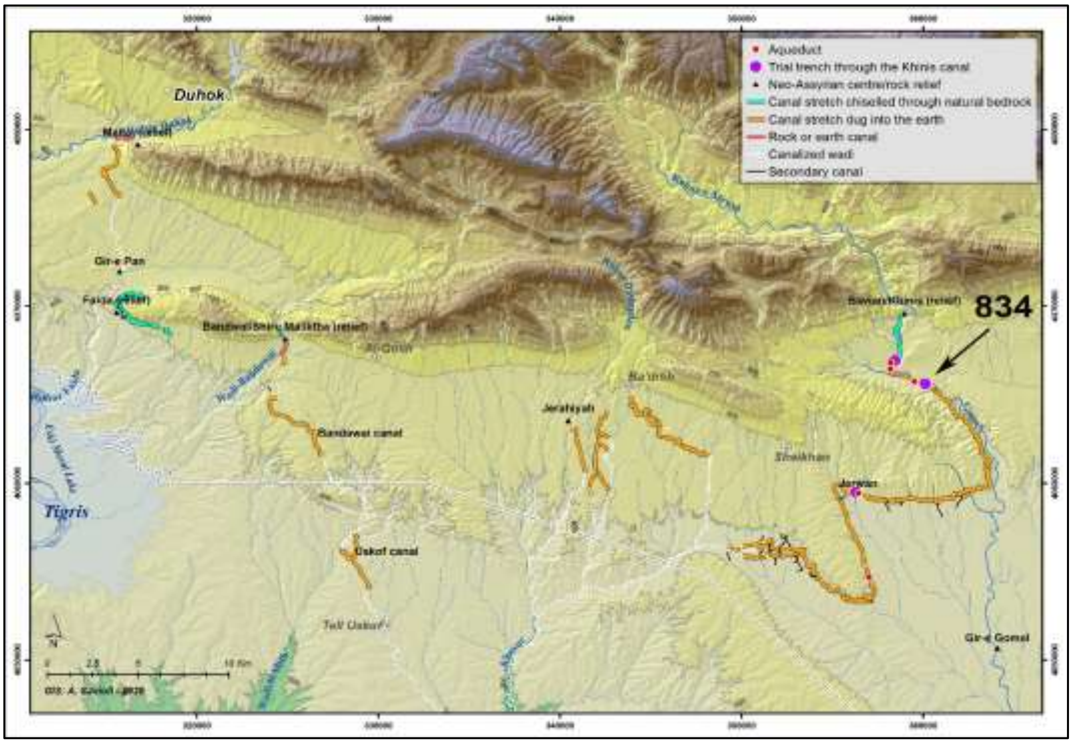

Figure 6 More detailed look on Faida, Maltai, Khinis, Bandawai, Uskof and Ba'dreh canals, provided by the LoNAP team.

Both cross-section 834 and 133 are of roughly rectangular shape, with the former having a bottom width of 4,8 m, reaching 8,3 m at the top, and a 1,5-1,6 m height from the canal bottom. The latter has a bottom width of 6 and top width of 6,25 m, while its maximum water depth is assumed to range between 1,5 and 3,8 m (Morandi Bonacossi, 2019). While the three cross-sections 834, 133 and Jerwan are presented below in Figures 7, 8, and 9. Bed material consists of natural bedrock (primarily limestone) in the upstream parts, with earthworks downstream, excluding the aqueducts which are characterized as masonry (limestone based) (Morandi Bonacossi, 2019). Detailed data on bed slopes is unavailable, therefore a general estimate of 0,9 m/Km is assumed throughout the canal (Ur, 2005).

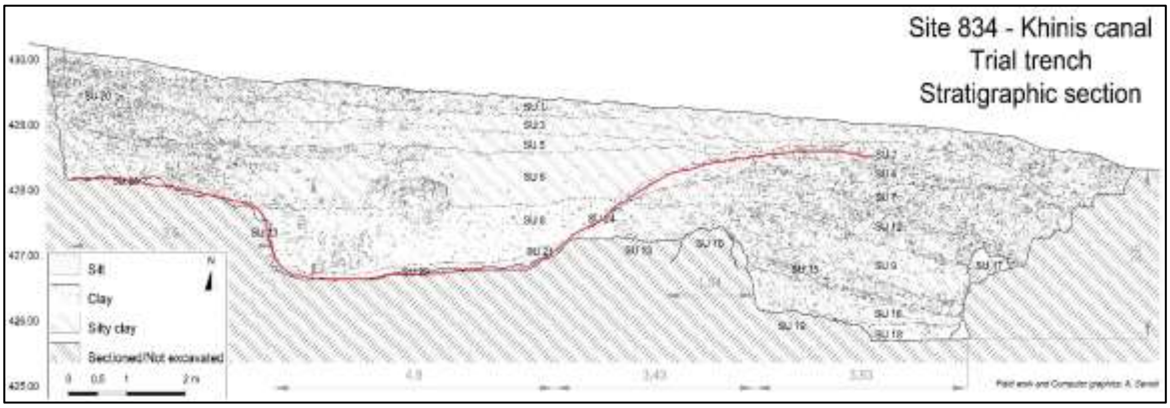

Figure 7 Trial trench 834 cross-section shape indicated by red line (Morandi Bonacossi, 2019).

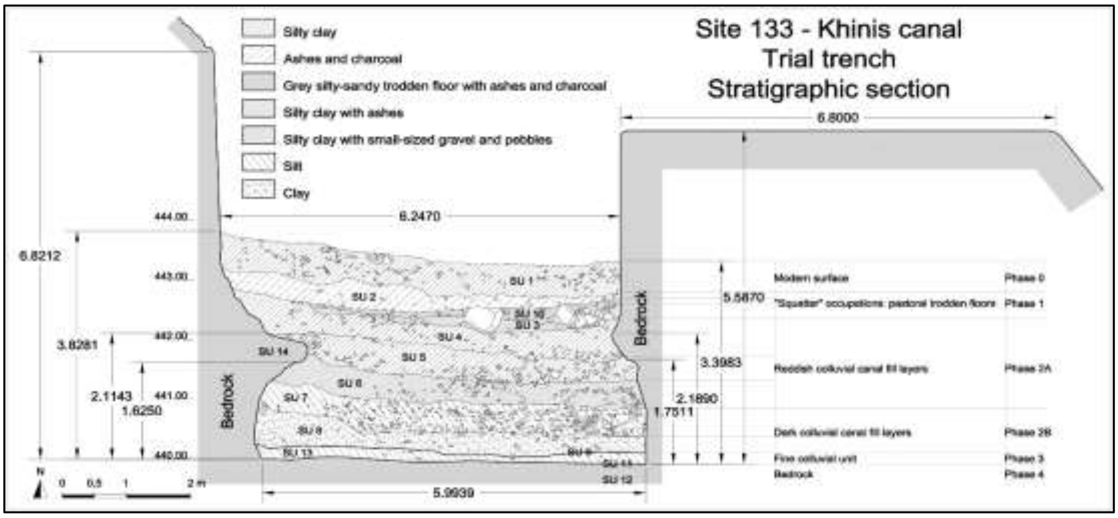

Figure 8 Trial trench cross-section 133 (Morandi Bonacossi, 2019).

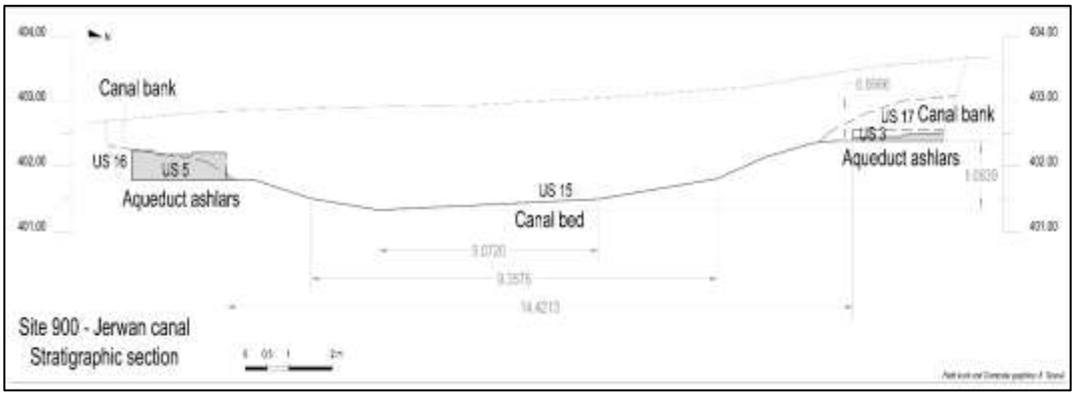

Figure 9 Jerwan Aqueduct trial trench 900 cross-section, by LoNAP team.

Bandawai has no available cross-section or detailed bed slope information, therefore a general slope of 0.9 m/Km is assumed. As can be seen in Figure 6, most of the canal bed is either shaped in earthen or canalized river segments, with the far upstream being an exception. This part consists of a tunnel chiseled through natural bedrock at the origin, met along its route by another tunnel feeding the far upstream Bandawai.

The **Ba'dreh-Jerahiyah** canals have no data other than their routes and bed material, a mix of earthen and canalized wadi, as shown in Figure 6.

Uskof, similarly to Bandawai, relies on general slope estimations of 1-1,2 m/Km and has no cross-section data. Canal bed material consists mostly of dug earth, with a large part of the watercourse joining the Khosr being a canalized river.

Kisiri has one identified offtake and just, like Uskof, lacks detailed data on bed slopes and cross-sections. A mean slope of 0,95 m/Km is assumed while the canal bed is made of earthwork (Ur, 2005).

Irrigable fields per canal

The identified offtakes along the main canals are often not sufficient to irrigate all irrigable area nearby, therefore additional secondary offtakes/canals were added to solve this issue. Worth noting is feeder channels were small (cross-sections) and got swiftly infilled by earth and eroded debris through the years. This made satellite recognition quite difficult, while it indicates that identified feeder channels represent only a small part of what existed. In Figure 10, the irrigable land along canals is shown together with existing and added offtakes. The number of existing and added offtakes is also shown in Table 1.

Table 1 Identified and added offtakes per area, recent (after this study modeled Faida) image processing by LoNAP has revealed 11 additional feeder channels in Faida.

Canal fields	Identified offtakes	Added offtakes
Maltai	1	4
Faida	4 (15)	0
Khinis upstream	0	3
Jerwan-Mumbarak	16	0
Ba’dreh	0	7
Khosr tributary	0	3
Bandawai	1	2
Uskof	0	2
Kissiri-Nineveh	1	2

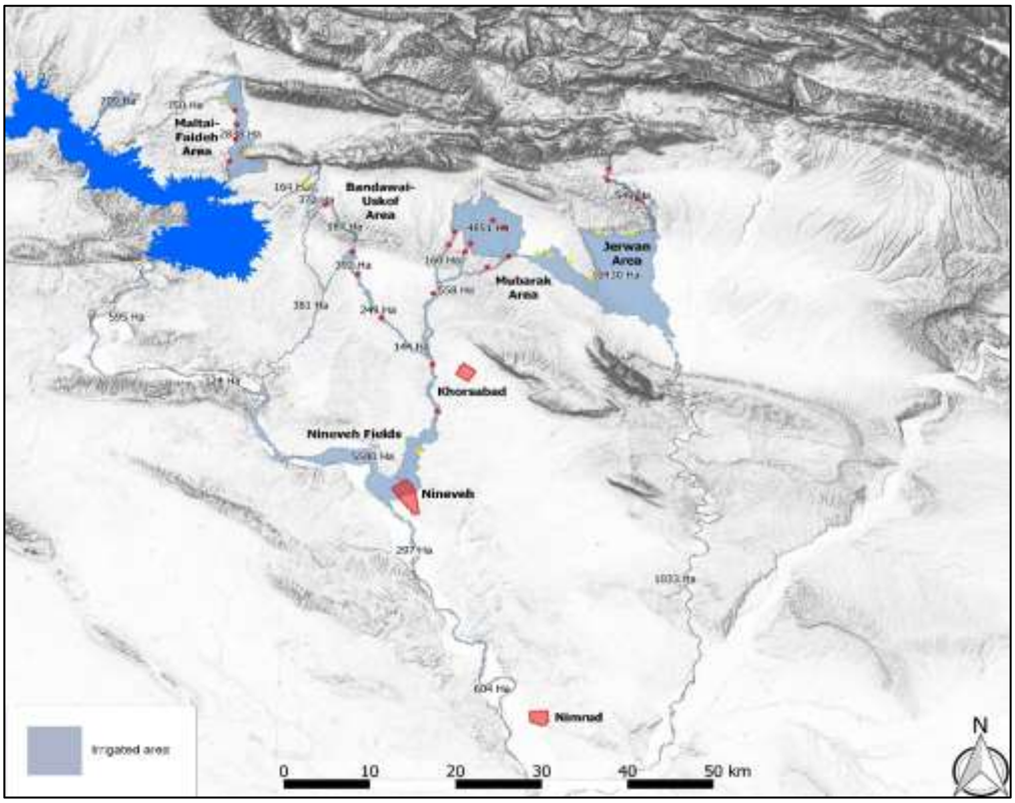

Figure 10 Irrigable land of both Regional and Local systems, with orange dots indicating identified offtakes and red the additional ones.

Climate-Soil

The Neo-Assyrian mainland resided between the cities of Assur, Nineveh, and Arbela, forming a triangle region and experiencing 90-95% of its annual precipitation during

November-April (cool season) through Mediterranean cyclonic systems. Today, the Neo-Assyrian heartland lies in a zone of high inter-annual variability, above the 200-300 mm isohyets delineating the "uncertainty zone" (frequent crop failure) for rain fed farming. (Sinha et al., 2019) reconstructed the region's hydroclimate of the past 4000-years, relying on δO_{18} and δC_{13} measurements as proxies for wetness, allowing linking to rainfall anomalies. The results correlate drier intervals of the Neo-Assyrian period (700-660 BCE) to values observed within the 1979-2007 datasets of the region. This providing a meaningful comparison of the Assyrian megadrought with post 1980 CE droughts (for years 1999-2000 and 2007-2008), where the largest reduction in cool-season precipitation was observed at around 60 % (Sinha et al., 2019).

Similarly, precipitation and temperature data from 1979-2010 are used as input in the crop growth simulation software in this thesis. Faida village, Nineveh, and a point in the Navkur plain (shown in Table 2) are selected as these represent different and relevant rainfall and temperature patterns and quantities. Precipitation, minimum and maximum temperature data used are of daily, 0,5° X 0,5° temporal and spatial grid resolution, respectively from year 01/01/1979 until 31/12/2010. These data were retrieved from the National Oceanic and Atmospheric Administration's website CPC Global Temperature/Precipitation data provided by the NOAA/OAR/ESRL PSL, Boulder, Colorado, USA, from their Web site at https://psl.noaa.gov/ in NetCDF format, which were processed to Excel datasets through a few of simple Python scripts.

Table 2 Coordinates used for precipitation and temperature data.

Names	Latitude and Longitude
Faida	36.748185°, 42.933191°
Nineveh	36.339927°, 43.128763°
Navkur plain	36.624583°, 43.431370°

The most reliable data for soil types in the above points are found in the 1960 study from Iraq's Ministry of Agriculture (Buringh, 1960), before excessive modernization of the region took place. Soils in Nineveh, the northeastern Navkur plain and South of Dohuk (Faida, Bandawai) region, are mainly brow-red brown soils with occasional deposits of limestone and gypsum existing in the vicinity. Nineveh soils are characterized as deep, varying from 2 to 4 m, and loamy - fairly to highly fertile soil types with non-existent salinity (Buringh, 1960; Morandi Bonacossi, 2018). The Navkur plain and Faida- Bandawai regions are mentioned as silt loams with depths of 1,5 - 3 m with high fertility (Buringh, 1960).

Rainfall, temperature, and soil types will be used as input for the crop growth simulating AquaCrop model. User-based parameters, such as sowing rates, growing seasons, and yields, will also be included.

Crop Growth Simulation

One of the reasons water systems can be beneficial for an empire is their ability to provide water for irrigation needs of crops and potential transportation of harvests to the capital or regional capitals. Assuming capable water managers organize and oversee operation (without specifying who these managers were), this would benefit both local and Nineveh's harvest yields in the case of Neo-Assyria, while friction-less transport of grain would greatly improve economic commerce of the region.

For the Assyrian empire, barley and wheat appear as the most dominant crop throughout the region. Although orchards existed, they presumably were not the main in terms of produced crop harvests, as water demand is considerably higher than cereals. Neo-Assyrian records of crop data in any form are hard to come by, hence relying on Old Babylonian/Middle Bronze Age II period (1800-1750 BCE) data is inevitable given our current knowledge. These data propose, primarily for Mari and the northeastern Euphrates plain, a dominance of barley as crop of choice over wheat at around 90% (Reculeau, 2011). Nineveh and nearby areas are assumed to have used similar crops as the fields in the North of Mari, due to their proximity and annual precipitation/temperature similarities. This is not the case for fields irrigated by Faida and Khinis- Jerwan, as they experience significantly higher rainfall and lower winter temperatures. (Morandi Bonacossi, 2018) also suggests that barley followed by wheat were the dominant crops of these regions, although no evidence on harvest yields or sowing data are available. The modelled crop of choice in this thesis is barley, which differs from wheat primarily in temperature, water stress tolerance and archeological data availability. Barley sowing rates and harvest estimates are available in higher quantity and with lower uncertainty through the Middle Assyrian period (Reculeau, 2011).

Assyrian Barley

Barley's two most important shapes come in two-row or six-row, with the latter being a product of mutations most likely through selective breeding. As mentioned by the Food and Agriculture Organization (FAO), two-row barley contains two rows of seeds, while six-row barley has six in total, leading to the straightforward assumption of a reference harvest index value of 1/3 for two-row, when compared to six-row.

Growth cycles recorded in the Middle Assyrian region of Euphrates suggesting barley planting happening in early fall and harvesting around late spring – as rainfall amounts and temperatures favor this period over the rest of the year (Reculeau, 2011). Cycles from early spring to early summer could be possible, given water availability and winter stresses in the norther fields, however. FAO mentions a few barley varieties (such as winter, spring and Mediterranean), with cycles of the last two in the range of 91-96 and 137-150 days each. The Mediterranean cycle length seems to correlate with fall sowing; the spring cycle links with the remaining cycle proposed. Sowing rates are recorded in qu/iku, representing volume/weight per area, with 30 or 35 qu/iku representing most likely average use rates (Reculeau, 2011). Conversions of qu/iku in kg/ha are made based on the Middle Assyrian value of iku being equal to 0,42 ha. This value is assumed to remain stable throughout the Neo-Assyrian period, while qu values of 0,5 or 0,65 kg are deemed equally possible (Reculeau, 2018). Yield rates are expressed in seed per yield, with the highest records reaching 1:10. This is used as a reference yield rate to calibrate the harvested yield produced by the model AquaCrop.

Irrigated Area to Harvest and Water Demand

Converting hectares of irrigated land to crop water demand and potential yield will take place with the modelling tool AquaCrop, provided by FAO. It incorporates weather, soil, groundwater, irrigation schedules, crop parameters and field management effects on potential water demand and yield. The irrigated area is provided by (Morandi Bonacossi, 2019), based on gravity-irrigated land calculations through GIS. AquaCrop has a library of crops that includes six-row barley; therefore, some adjustments are required to recreate an Assyrian crop, closer to the two-row variety. The reference harvest index is assumed at 1/3 of the six-row value, as stated above, and growth cycles of 96 and 150 days are assumed for spring and fall sowing respectively, while precipitation and minimum/maximum temperature time series are obtained for fields in Nineveh, Faida, Navkur to incorporate potential differences in resulting water demand. Soils are separated in fields around Nineveh's and Navkur-Faida's, which are considered at a depth 3 and 2,25 m each. These fields are characterized as loamy and silty loam, respectively, with no salinity for all fields and high to extremely high fertility. Perhaps a reduction in hydraulic conductivity due to increased clay percentages in Faida and Navkur fields would be possible, but this is not included.

Groundwater table depths are rather deep, ranging from 10 to 40 m below surface, therefore no capillary rise can introduce salts in the soils or significantly interact with the crops. Lastly, water productivity relative to CO_2 concentrations are adjusted to account for reduced amounts around 700 BCE – this is the most uncertain parameter. It was be used to calibrate the modeled maximum harvest with recorded seed/yield rates. Through AquaCrop, net water demand is calculated per unit of surface area, with rain and temperature of growing season highly influencing its values. Harvested yield depends on the above parameters and the percentage of water demand met, which is ultimately a result of canal network capabilities, along with priorities in water allocation.

AquaCrop

Below the model's parameters: Climate, Crop, Management, Soil and Simulation are described. Explanation for choices is provided. The main menu of AquaCrop is shown in Figure 11.

Figure 11 AquaCrop main menu, FAO software.

Climate parameters consist of precipitation, min/max temperature, potential Evapotranspiration (ET0) and CO_2 concentration, as shown in Figure 12.

Figure 12 Climate parameter inputs AquaCrop.

Two years are chosen to simulate, based on Nineveh's max and min annual precipitation from 1979-2010: a wet and a dry year. The former is 1980 with 494 mm/yr, while the latter is 1999 with 128,5 mm/year (one of the years mentioned by (Sinha et al., 2019) showing similarities in stable isotopes markers ($\delta_{18}O$) and ($\delta_{13}C$) in comparison with the so-called Neo-Assyrian "Megadrought"). Crop failures were also reported in high frequency during the dry year in modern Iraq. Temperature min and max that were used correspond with the rainfall years 1980 and 1999.

ET0 measurements are unavailable, therefore are calculated by AquaCrop using mean altitude above sea level, latitude, air temperature, air humidity, net radiation, and wind speed. The last three parameters are calculated indirectly based on the first three, while altitude is obtained from Google Earth Pro along with the latitude coordinates from Table 2. CO_2 concentrations around 700 BCE were much lower than the present day, but no reliable data could be found to estimate these values. A choice of creating a CO_2 file with one constant value (using the build in CO_2 files lowest value for year 1950) solves the issue of AquaCrop automatically selecting CO_2 values corresponding to modelled years (1980,1999).

The next element is Crop, containing assumptions to bring the six-row barley model values closer to the Assyrian two-row variety. Sowing rates converted from qu/iku to kg/ha range from 35,71 kg/ha to 57,16 kg/ha. For simplicity and due to no real evidence allowing any guiding, the 35,71 kg/ha of seeds is chosen. This also serves as a conservative estimate. After discussions with Professor Herve Reculeau and consulting (Reculeau, 2011), spring and autumn season sowing dates were chosen, at 7th of March and 7th of November, respectively. The maximum obtained yield was decided at 1 seed producing 10 grains based on (Reculeau, 2011) (1 for 9 was the value in Middle Assyrian records). Growing degree days are used instead of calendar days, as these provide variable amounts of growth based on air temperature, with lower and upper limits at 0 and 15 ^{o}C. The next important parameters are crop water productivity and harvest index, these are used to calibrate the dry harvest. The reference harvest index was 33%, which, as mentioned above, is reduced to 11%. Crop water productivity (WP*) is a factor affecting yield formation (based on transpired water), which depends on the atmospheric CO_2 concentrations. In order to counter a) the unknown $C0_2$ concentrations around 700 BCE and b) AquaCrop selecting different concentrations from its build in file (spanning 1950-2020), a constant concentration file is created as mentioned above. Since decreasing the reference harvest index was not enough to comply with documented maximum yields from Middle Assyrian records (1 seed to 10 grains), and the true value of WP* is unknown it is calibrated so that harvest meets documented maximum values for the wet year Spring. More details are presented in Figure 13.

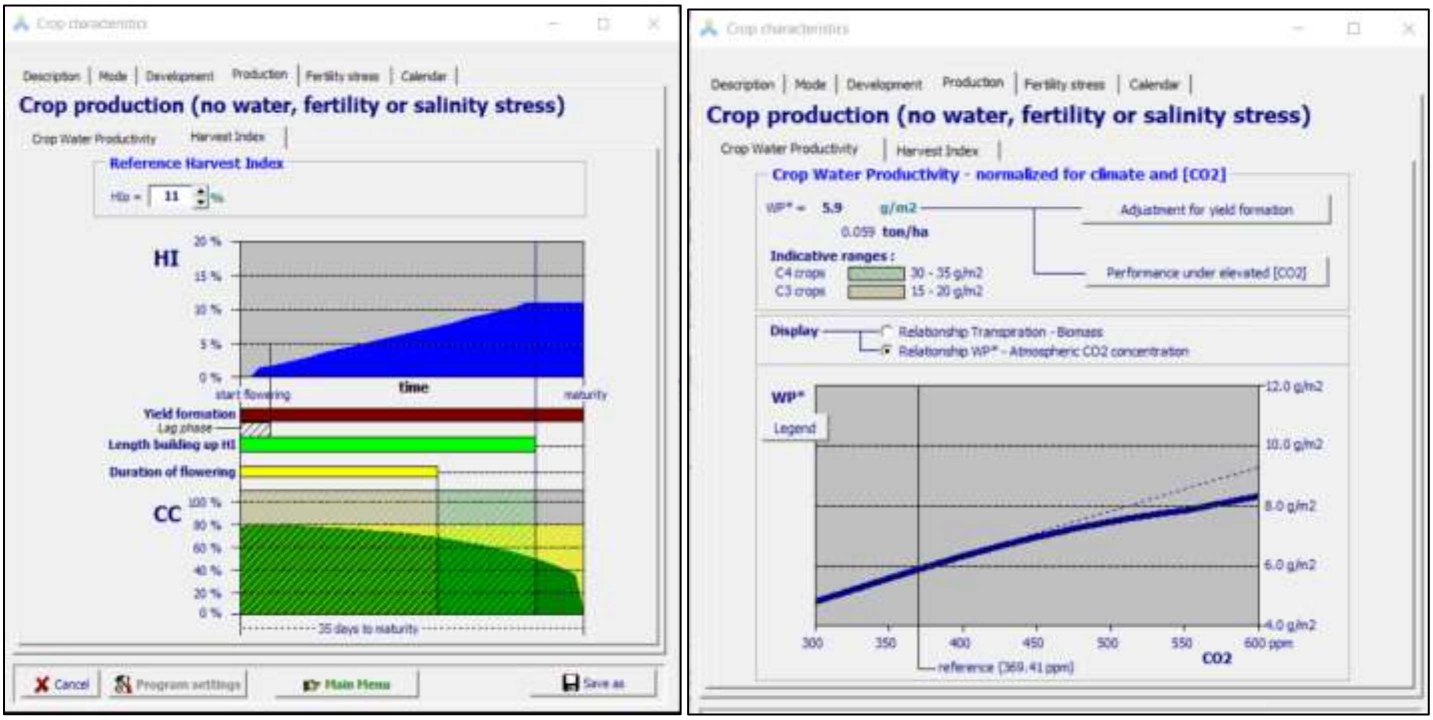

Figure 13 Left screen presenting Harvest index, while right screen crop water productivity.

Management choices consist of two sections ("Irrigation" and "Field"), with the first providing an estimate for irrigation needs and the latter defining field maintenance and its effects. Irrigation can be estimated as a continues water demand or defined by conditions, such as the amount in mm and the threshold at which to irrigate. Three amounts are experimented with in this thesis, with 20, 30 and 40 mm per irrigation event, to rank their performance and chose one as a condition for the flow simulating model (Sobek). The threshold at which the model irrigates is when Readily Available Water (RAW) drops at or below 50%, while the method is surface irrigation and more specifically by furrows. In Figure 14, a view of the irrigation schedule with these conditions is shown.

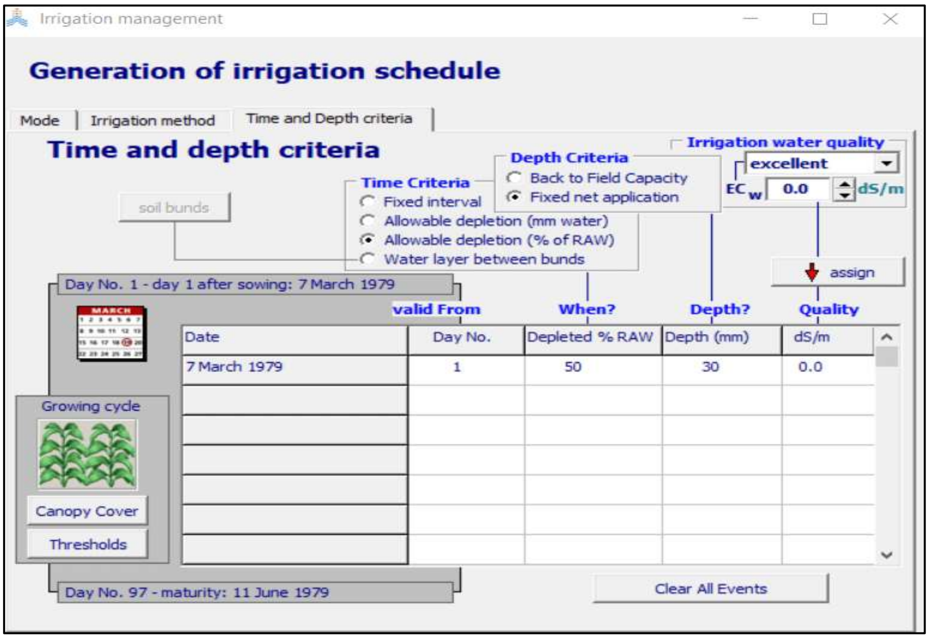

Figure 14 Irrigation schedule menu, as provided by AquaCrop.

Field management is divided in two: the capital's fields receive more attention and the Navkur-Faida are characterized as slightly more fertile. These are represented by a 17 and 6 % decrease in soil fertility, for Nineveh and Navkur-Faida fields. Field surface processes, such as furrow irrigation, affect the surface runoff – increasing it by 5% for both lands. Finally weed management considers 5% infestation at the beginning of the season, which in the case of Nineveh decreases to 3% until the end.

The Soil section consists of the soil profile and groundwater parameters, taken from the **Climate-Soil** paragraph. Nineveh soils are characterized as loamy with a depth of 3 m, while Navkur-Faida soils are silty loam with a depth of 2,25 m. In Figure 15 more details for both soils are presented. Groundwater, as mentioned above, is found between 10 and 40 m depth, therefore considered as deep with no effect on crops.

The Simulation inputs are used to define the start date of the simulation and its initial conditions. For a more realistic simulations, since no soil water balance data are available, the 15th of August is chosen as the start date, with the soil water % assumed to be at permanent wilting point PWP. AquaCrop calculates the soil water balance accounting for rainfall, evaporation, runoff, resulting in a better estimate of soil water conditions at planting. Wet years simulations starting years are 1980 in Spring and 1979 for Autumn runs, while Dry are both in 1999.

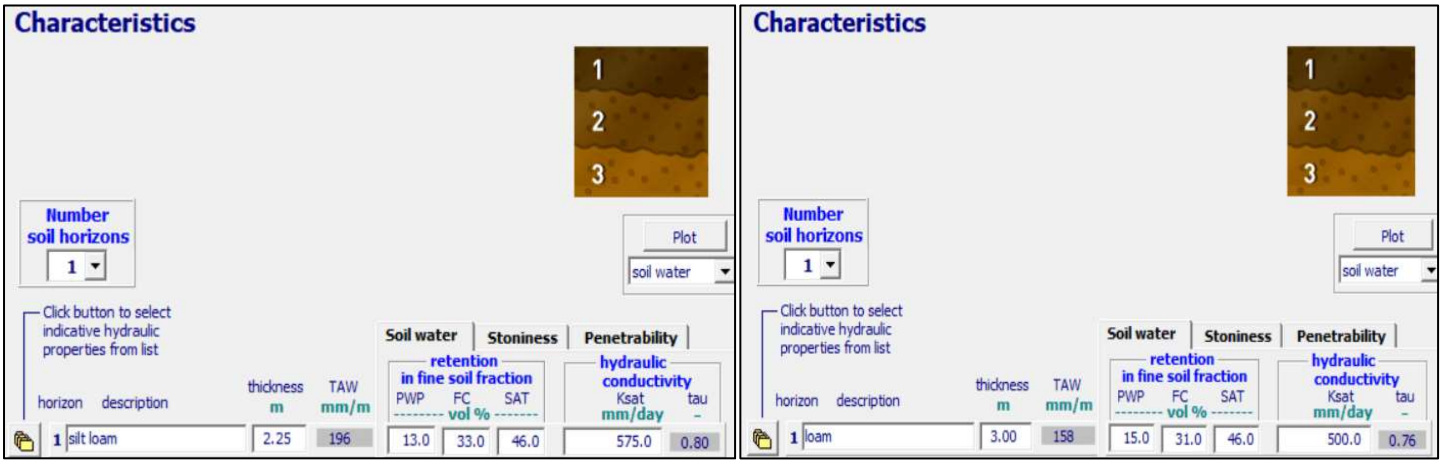

Figure 15 Total available water TAW, hydraulic conductivity for the left Navkur-Faida soil and right Nineveh's soil.

Results of the simulations runs produce the required sequence of irrigation events, from which corresponding available days to irrigate are created. In Table 3 below, the harvested yields over seasons and years are presented, showing small variances between delivery amounts over years, but significant differences in seasons.

Table 3 Dry harvest yield for Rainfed, Net water requirement and 20-30-40 mm delivery schedules during Spring-Autumn seasons and Wet-Dry years.

		Wet year					Dry year				
	Deliver pre event (mm)	**40**	**30**	**20**	**Net Requirment**	**Rainfed**	**40**	**30**	**20**	**Rainfed**	**Net Requirment**
Nineveh fields	**Spring**	204	203	203	207	146	203	203	203	DEAD	203
	Autumn	354	355	353	358	DEAD	366	366	365	DEAD	367
Navkur fields	**Spring**	217	218	218	219	203	216	216	216	DEAD	216
	Autumn	348	350	349	364	354	364	367	365	DEAD	367
Faida fields	**Spring**	218	218	218	219	192	218	218	217	DEAD	219
	Autumn	366	366	365	377	346	337	336	336	DEAD	376

By running AquaCrop simulations with the three delivery event amounts (20, 30, 40 mm), 12 irrigation schedules (per location) are obtained considering wet/dry years and spring/autumn seasons. For each area, season and year, a schedule of consecutive irrigation events is produced by AquaCrop and documented. A column is created, featuring the duration in days available to irrigate, based on three consecutive event dates. For example, by taking any three consecutive events, calculating the duration in days between them and dividing by two, the amount of irrigation cycles completed before the third (consecutive) begins. This provides a column of available days to deliver 30 mm per hectare (for each scenario), from which the minimum days are chosen to represent that scenario's available days to irrigate. Tables 1 through 4 in the ANNEX show these calculations and elaborate on them.

Table 4 below presents the minimum number of days, summarizing the tables in the ANNEX. These provide a temporal boundary condition, limiting the flow simulation model (Sobek), with their number depending on the year, season, location, and delivery amount used. The 30 mm delivery per event is chosen to be modeled with Sobek (the flow simulation model used). The choice is based on this amount providing less labor demands (as in high number of events) compared to the 20 mm scenario. The 30 mm scenario shows slightly higher number of events than the 40 mm one, but lower total water amounts are needed for Nineveh in dry years.

Table 4 Maximum days to complete an irrigation event along with total amounts in (mm/ha) and number of events per year and season.

			Max days (Total mm)			Number of events	
	Deivery amount (mm)	Faida	Navkur	Nineveh	Faida	Navkur	Nineveh
Wet Year	20	3 (220)	2.5(200)	3(240)	11	10	12
Spring	30	5(210)	5(210)	4.5 (270)	7	7	9
	40	7,5(200)	7,5 (200)	6(240)	5	5	6
Autumn	20	9,5 (100)	6 (120)	2.5 (160)	5	6	8
	30	10 (120)	9 (150)	4.5 (150)	4	5	5
	40	10 (120)	10 (200)	10 (160)	3	5	4
Dry Year	20	1 (480)	2.5 (440)	1 (460)	24	22	23
Spring	30	4 (480)	4 (420)	4 (450)	16	14	15
	40	5,5 (480)	5,5 (440)	5,5 (480)	12	11	12
Autumn	20	1 (360)	1 (320)	1 (300)	18	16	15
	30	4 (360)	4.5 (330)	5.5 (330)	12	11	11
	40	5.5 (360)	5.5 (320)	5.5 (360)	9	8	9

After running Sobek, a set of water amounts with coverage percentages is obtained for each year (wet, dry), season (spring, autumn) and control scenarios (further details on these in the Sobek section). These percentages and amounts will be used as input for the Irrigation section of Management in AquaCrop, to derive the final estimation on dry harvest yields for the above-mentioned combinations of scenarios. Assuming timing of events remains unchanged, the amount delivered will be multiplied by the coverage percentage corresponding with the scenario and location chosen. Additionally, calculating days between events as available time to irrigate and dividing them with the least number of days shown in Table 4 for the 30 mm scenario, produces a fraction. Multiplying this fraction with the percent coverage leads to an improved estimation of available water reaching the fields. Tables 5 and 6 below show the detailed irrigation schedules and above-mentioned calculations for the 30 mm delivery amount.

Table 5 Dry year 30 mm delivery amount irrigation schedule, presenting available days to irrigate for each event and its fraction to multiply with coverage percentage.

Nineveh		**Spring**	**Navkur**			**Faida**		
30mm Sequence	Irrigation Days available	fraction coverage achieved	30mm Sequence	Irrigation Days available	fraction coverage achieved	30mm Sequence	Irrigation Days available	fraction coverage achieved
205	1	0.25	205	1	0.25	205	1	0.25
206	8	2	206	11	2.75	206	8	2
214	25	6.25	217	27	6.75	214	33	8.25
239	8	2	244	6	1.5	247	4	1
247	6	1.5	250	6	1.5	251	5	1.25
253	4	1	256	5	1.25	256	4	1
257	4	1	261	4	1	260	4	1
261	5	1.25	265	5	1.25	264	4	1
266	5	1.25	270	4	1	268	4	1
271	5	1.25	274	4	1	272	5	1.25
276	5	1.25	278	6	1.5	277	5	1.25
281	5	1.25	284	6	1.5	282	5	1.25
286	4	1	290	6	1.5	287	5	1.25
290	6	1.5	296			292	6	1.5
296						298		
30mm Sequence	Irrigation Days available	fraction coverage achieved	**Autumn** 30mm Sequence	Irrigation Days available	fraction coverage achieved	30mm Sequence	Irrigation Days available	fraction coverage achieved
83	1	0.142857	83	1	0.166667	85	1	0.181818
84	10	1.428571	84	8	1.333333	86	7	1.272727
94	17	2.428571	92	5	0.833333	93	4	0.727273
111	24	3.428571	97	7	1.166667	97	7	1.272727
135	55	7.857143	104	14	2.333333	104	11	2
190	20	2.857143	118	110	18.33333	115	18	3.272727
210	10	1.428571	228	7	1.166667	133	93	16.90909
220	10	1.428571	235	11	1.833333	226	7	1.272727
230	6	0.857143	246	11	1.833333	233	10	1.818182
236	8	1.142857	257	7	1.166667	243	5	0.909091
244			264			248	9	1.636364
						257		

Table 6 Wet year 30 mm delivery amount irrigation schedule, presenting available days to irrigate for each event and its fraction to multiply with coverage percentage.

	Nineveh			**Navkur**				**Faida**		
Spring	30mm Sequence	Irrigation Days available	fraction coverage achieved	30mm Sequence	Irrigation Days available	fraction coverage achieved		30mm Sequence	Irrigation Days available	fraction coverage achieved
	53	6	1.5	59	9	1.8		52	10	1.666667
	59	5	1.25	68	8	1.6		62	7	1.166667
	64	5	1.25	76	6	1.2		69	7	1.166667
	69	6	1.5	82	5	1		76	6	1
	75	3	0.75	87	5	1		82	5	0.833333
	78	6	1.5	92	9	1.8		87	5	0.833333
	84	5	1.25	101				92		
	89	7	1.75							
	96									
Autumn										
	30mm Sequence	Irrigation Days available	fraction coverage achieved		30mm Sequence	Irrigation Days available	fraction coverage achieved	30mm Sequence	Irrigation Days available	fraction coverage achieved
	1	1	0.1	1	11	1.222222		1	15	1.5
	2	8	0.8	12	157	17.44444		16	149	14.9
	10	14	1.4	169	11	1.222222		165	9	0.9
	24	143	14.3	180	7	0.777778		174		
	167			187						

Sobek

Sobek is a numerical flow simulation model, containing various (numerical) modeling packages such as D-Flow 1D, D-RTC, D-Flow FM, D- Rainfall Runoff and D-Water Quality. From these modeling tools, D-Flow 1D and D-RTC are used, representing flow and real-time control.

- The D-Flow 1D module is designed for water flow modelling in open channels with various system complexity, cross-section shapes, boundary conditions and input sources. It simulates one-dimensional flow for shallow water, solving the full Saint-Venant equations with the assistance of the staggered grid numerical scheme (Deltares, 2019a).
- D-RTC or real-time control package is utilized by coupling with another flow package, in this case the D-Flow 1D. It has the responsibility of manipulating gate and weir heights, widths and openings based on time scheduling, or by conditions responding to discharge and water levels at chosen locations within the system (Deltares, 2019b).

The following sections will describe the transition from archeological data to their Canal Adaptations in Sobek, potential Control Scenarios, Input Sources and the evaluation parameter taken from AquaCrop, the water Delivery amount in available time.

Canal Adaptations in Sobek

Initially an important distinction between Local and Regional systems needs to be established. The Local system consists of the Faida and the Maltai canals, while the Regional includes Bandawai-Uskof, Khinis-Jerwan, Kisiri and parts of the Khosr river and one of its tributaries. Figure 16 show overviews of Local and Regional Systems – the scale does not allow showing all the details.

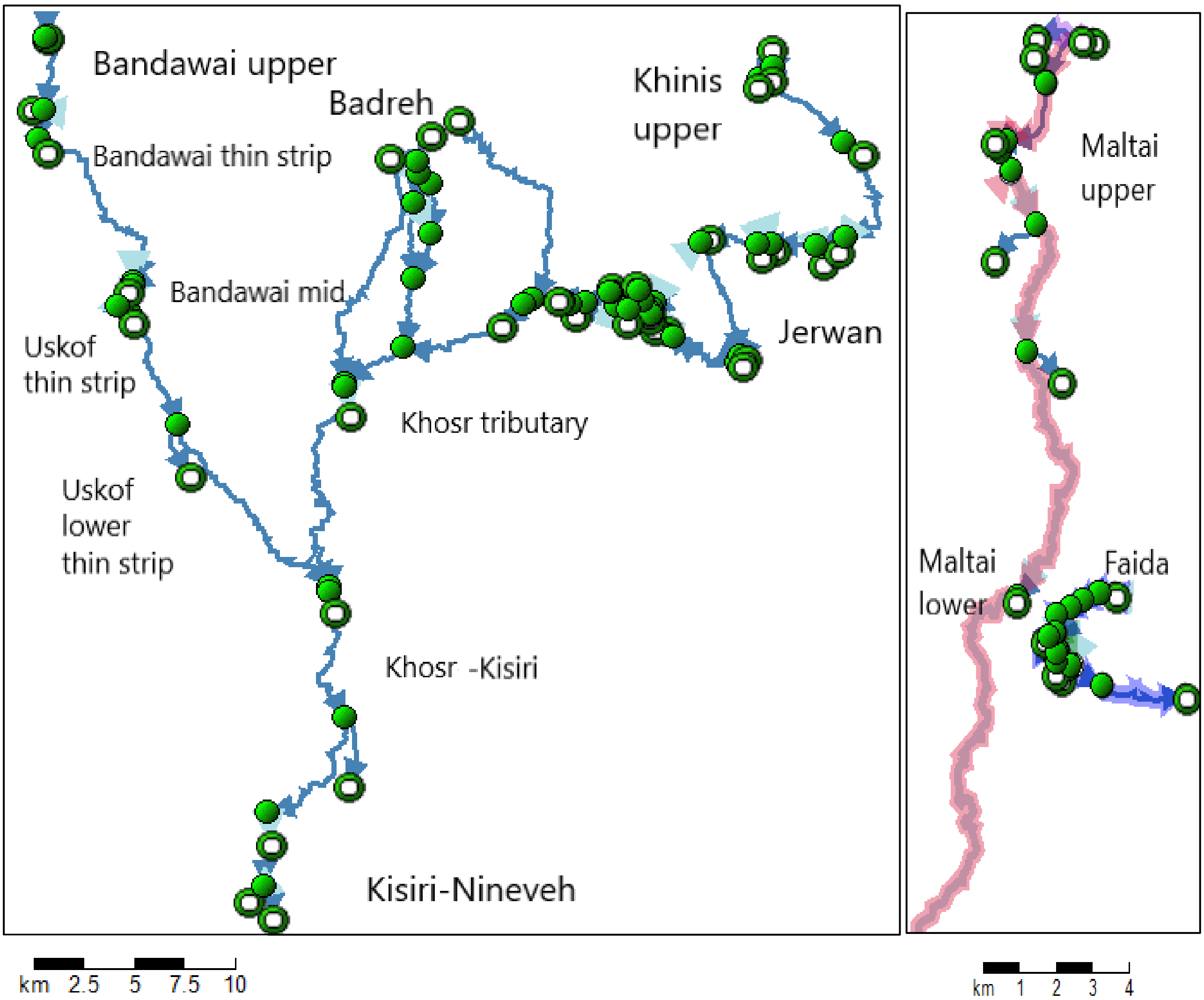

Figure 16 The Regional canal system is shown in the left while the Local on the right, green dots that are hollow represent canal origins or outputs (offtakes) while full green dots junctions between canals.

Slopes used in the main canals rely on (Ur, 2005) and their confirmation from (Morandi Bonacossi, 2019), except for Faida, which has more detailed data around its offtakes. Cross-sections used in the Local system rely on the Faida cross-sections, while for the Regional system, data for the Khinis and Jerwan aqueduct canal are provided by the LoNAP team. Values for the canals for slopes and number of cross-sections used are shown in Table 7 below.

Table 7 Canal slopes and archeologically identified cross-sections.

Canals	**Slopes (m/Km)**	**Cross-sections**
Faida	0.9	3
Maltai	4	0
Bandawai	0.9	0
Uskof	1	0
Khinis-Jerwan	0.9	3
Khosr tributary	0.9	0
Badreh	0.9	0
Khosr-Kissiri	0.95	0
Offtakes	0.9	0

Offtake canal slopes are assumed at 0.9 m/km, the lowest slope defined by (Ur, 2005), since no data on any of them was available.

Roughness used for canals depends on the LoNAP team's classifications, presented below in Table 8. The values shown are based on (Arcement & Schneider, 1989) and (Dr. Xing Fang, Department of Civil Engineering, 2000).

Table 8 Canal bed material types and their Manning roughness used in Sobek.

Canal bed types	**Manning Roughness (**s $m^{1/3}$)
Rock cut canal	0.011
Earthen canal	0.018
Rock or hearth canal	0.011
Canalized wadi/River	0.025
Aqueduct	0.022
Secondary canals	0.018

- Local system cross-sections: Figures 17 through 19 shown the three (archeologically identified) cross-sections and their adaptation in Sobek. These were also used to model the Maltai canal, with some slight alteration mentioned in the Detailed Canal Description.

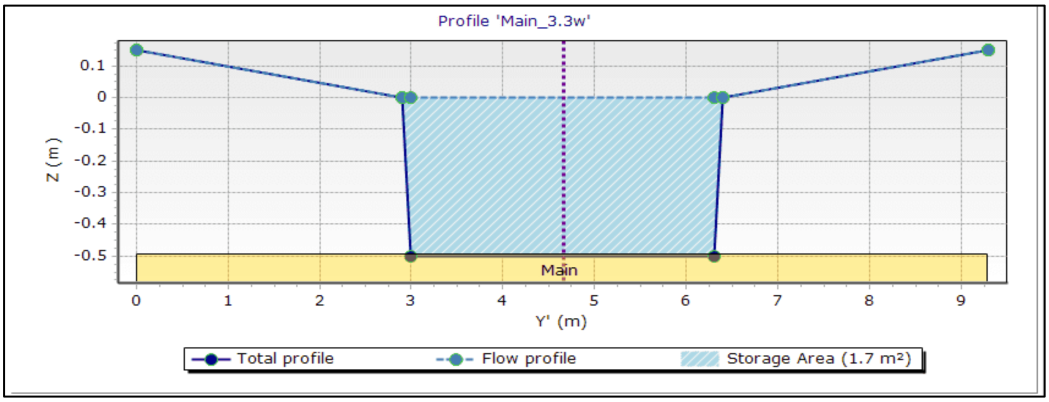

Figure 17 Faida canal 3,3 m width and 0.5 m water depth cross-section.

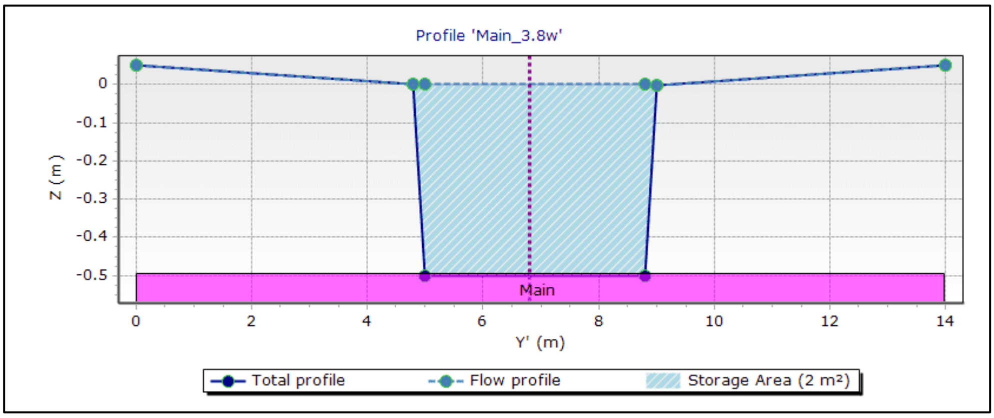

Figure 18 Faida canal 3,8 m width and 0.5 m water depth cross-section.

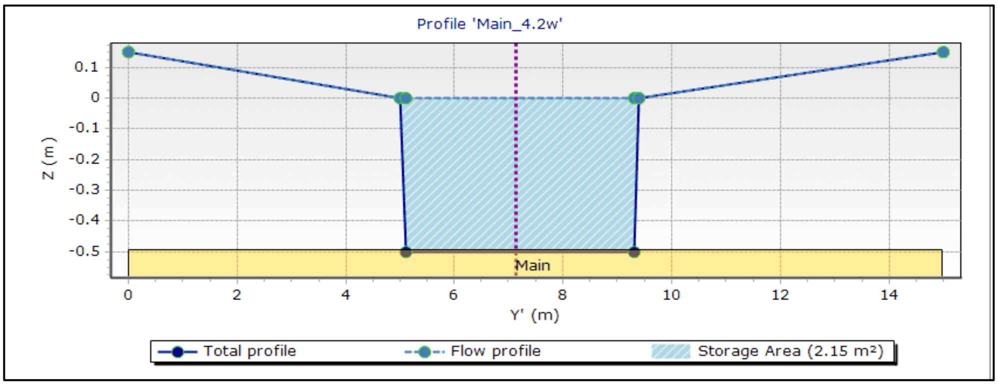

Figure 19 Faida canal 4,2 m width and 0.5 m water depth cross-section.

- Regional system cross-sections: Figures 20 – 22 represent the identified cross-section in the Regional system, with all of them residing in the Khinis-Jerwan canal sections. As for the Local system, these were used to estimate Bandawai, Uskof, Khosr-Tributary, Khosr-Kisiri and Kisiri-Nineveh cross-sections with some tweaks, elaborated further below.

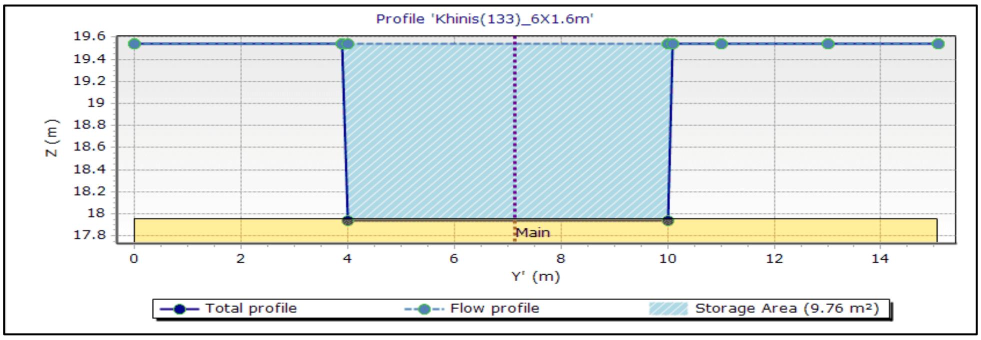

Figure 20 Khinis cross-section 133 6 m width and 1,6 m water depth.

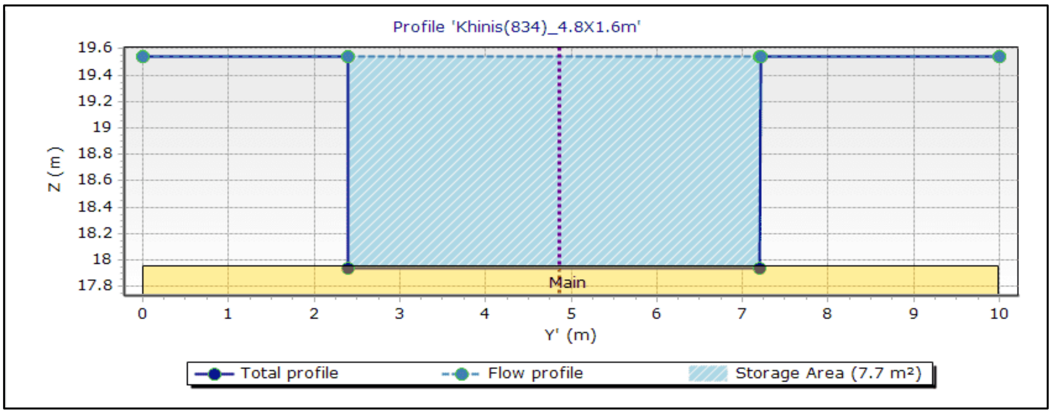

Figure 21 Khinis cross-section 834 4,8 m width and 1,6 m water depth.

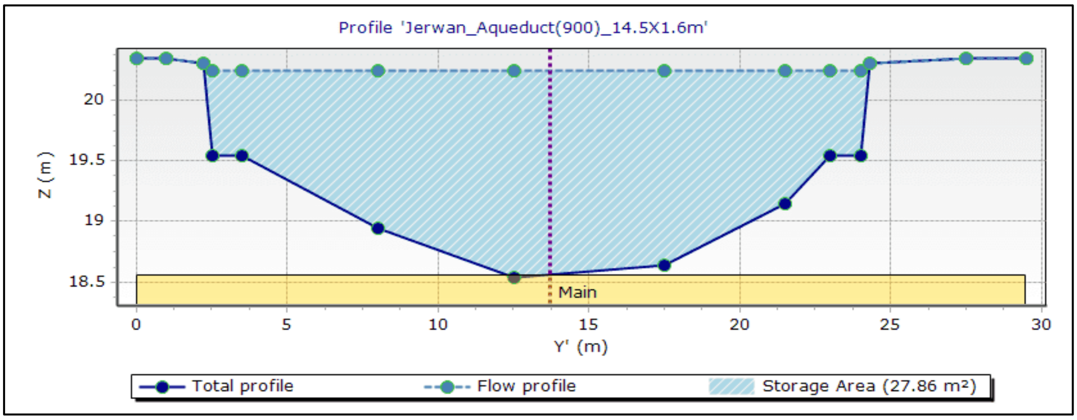

Figure 22 Jerwan aqueduct cross-section 14,5 m width and 2,5 m water depth.

Detailed Canal Descriptions

Worth noting is that most of the fields connected to canals lack the necessary offtakes to service their water allocation needs. Table 9 below present the offtakes deemed necessary to irrigate, the number of offtakes added and each canal's estimated irrigable land in hectares.

Table 9 Offtakes deemed necessary to irrigate, offtake number added and each canal's irrigable land in hectares, followed by required flow (m3/s) per offtake and area in the available days (Wet season). The last two rows show summaries for the Region and Local systems.

Canals	Offtakes	Offtakes added	Irrigable hectares	Flow per offtake and available days	Flow per area and available days
Maltai_upper	4	3	1495	0.216291	0.865162
Faida	4	0	1183	0.171152	0.684606
Bandawai_upper	1	0	90.86	0.063097	0.063097
Bandawai_up_thin_strip	1	1	187	0.261111	0.261111
Bandawai_mid	1	1	376	0.129861	0.129861
Uskof_upper	1	1	392	0.272222	0.272222
Uskof_lower	1	1	393	0.272917	0.272917
Khinis	3	3	549	0.127083	0.38125
Jerwan	16	0	10430	0.452691	7.243056
Koshr_tributary	3	3	675	0.15625	0.46875
Kisiri_Nineveh	3	0	5264	1.523148	4.569444
Khosr_thin_strip	2	2	316	0.137153	0.274306
Maltai_low	1	1	160	0.092593	0.092593
Badreh-Jerahiyeh	7	7	5011	0.497123	3.479861
Regional	39	19	23683.86	-	17.41588
Local	9	4	2838	-	1.642361

Faida is a rock-cut canal with four identified secondary canals, a mean slope around those is 0,77 m/Km and is made to mirror Figure 4. The placement of cross-sections and a detailed image of the canal is shown is Figure 23.

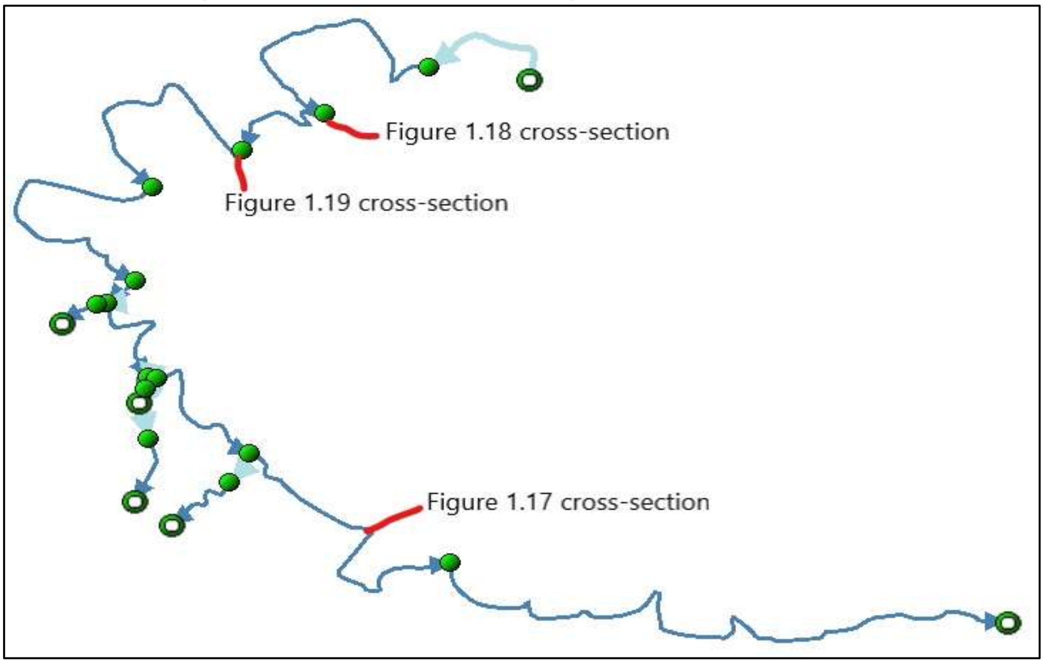

Figure 23 Faida canal cross-section placement.

Maltai uses the cross-section from Figures 18, until it switches to 19 with its roughness beginning as earthen transitioning to canalized wadi, based on the LoNAP team data. These are both designated on Figure 24. Four offtakes were added to be able to meet the irrigation needs.

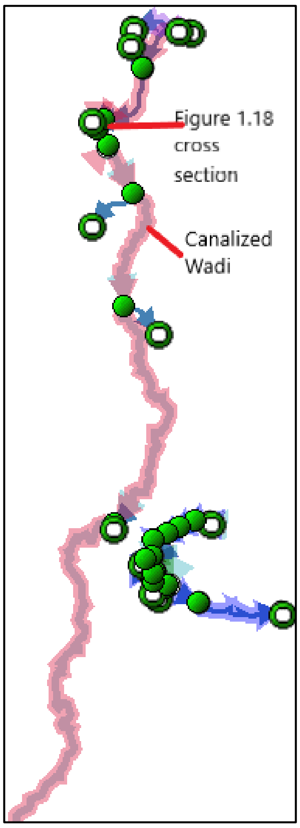

Figure 24 Maltai canal cross-section and roughness placement.

In its far upstream reaches, **Bandawai** is fed by two tunnels. With the help of Alberto Savioli from the LoNAP team, a cross-section and tunnel shape were estimated. Its Manning roughness is 0,025 s $m^{1/3}$, while the rest of the bed material is considered earthen. The linear transition from the tunnel cross-section to the 4,8 m width, 1,6 m height begins after the indicating “Bandawai tunnel” in Figure 26 and finalizes at 4,8 X 1,6m, with the cross-section in Figure 27 representing the rest of the canal: the Bandawai thin strip and mid-sections with earthen canal roughness.

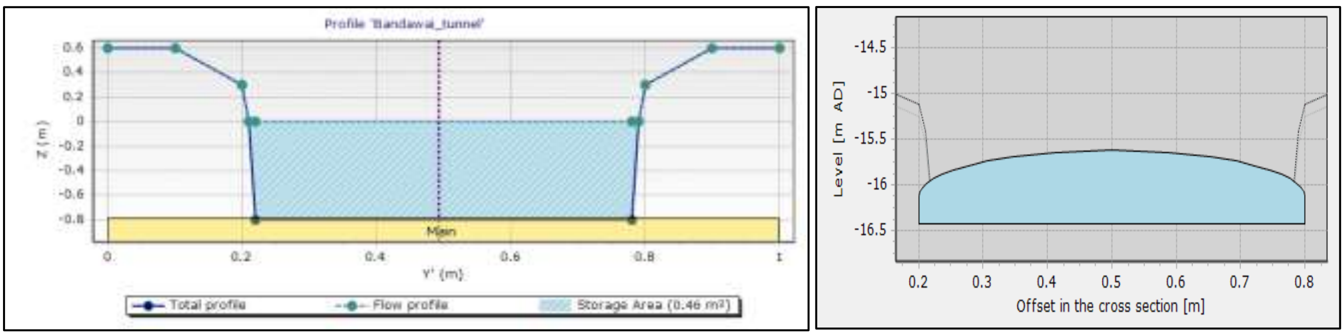

Figure 25 Bandawai tunnel cross-section on the left with the tunnel shape on the right, with 0.6 m width, 0.8 m height.

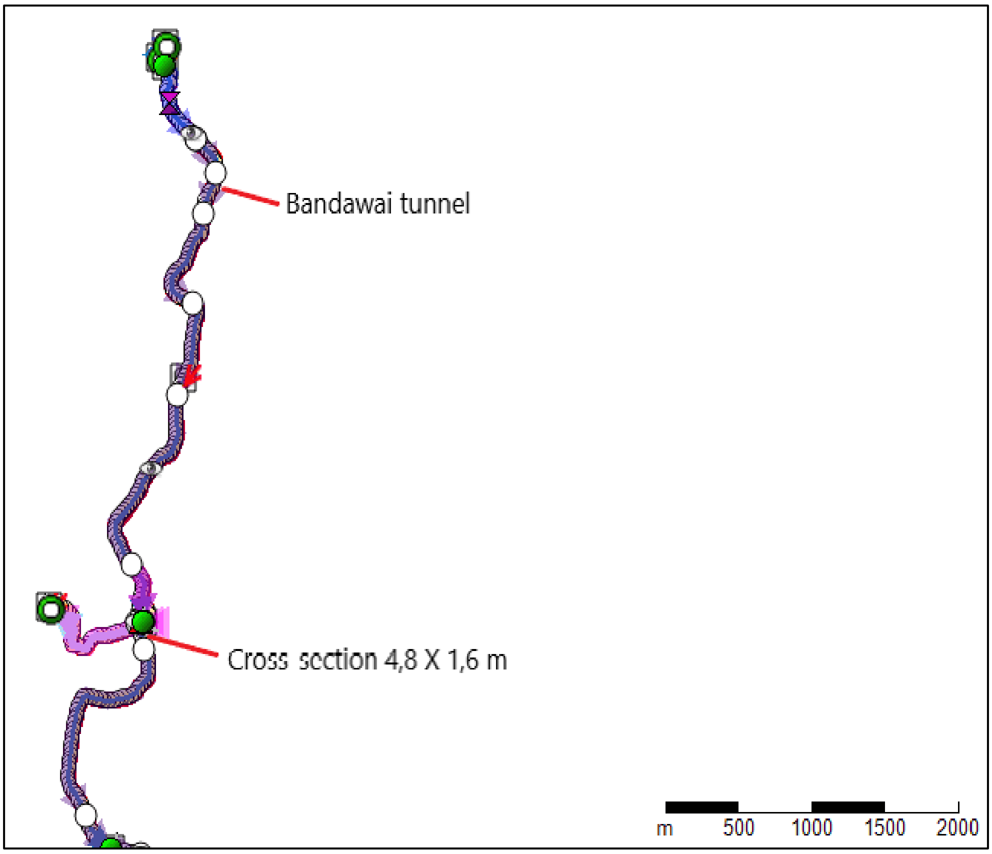

Figure 26 Bandawai upper section showing the extent of the tunnel cross-section and the beginning of the 4,8 X 1,6 m.

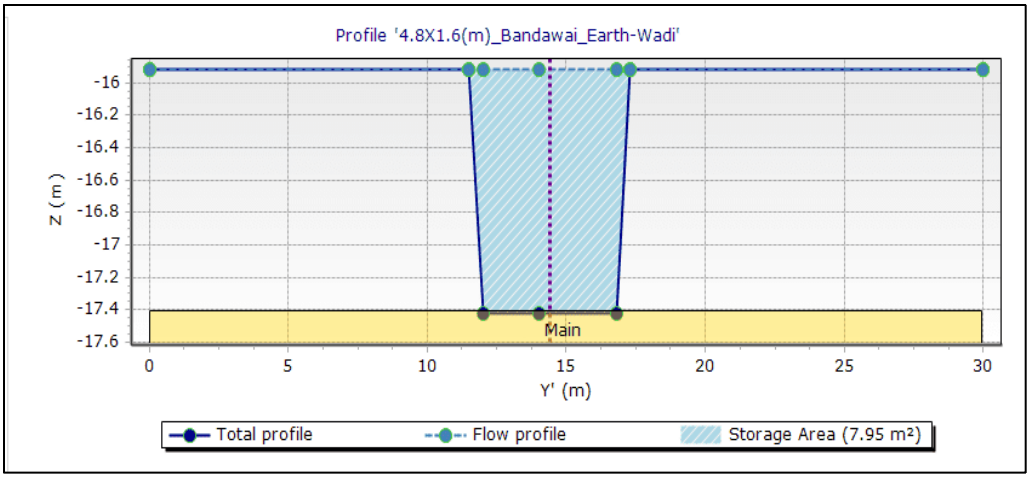

Figure 27 Bandawai cross-section used for earthen reaches emulating Khinis 834 cross-section.

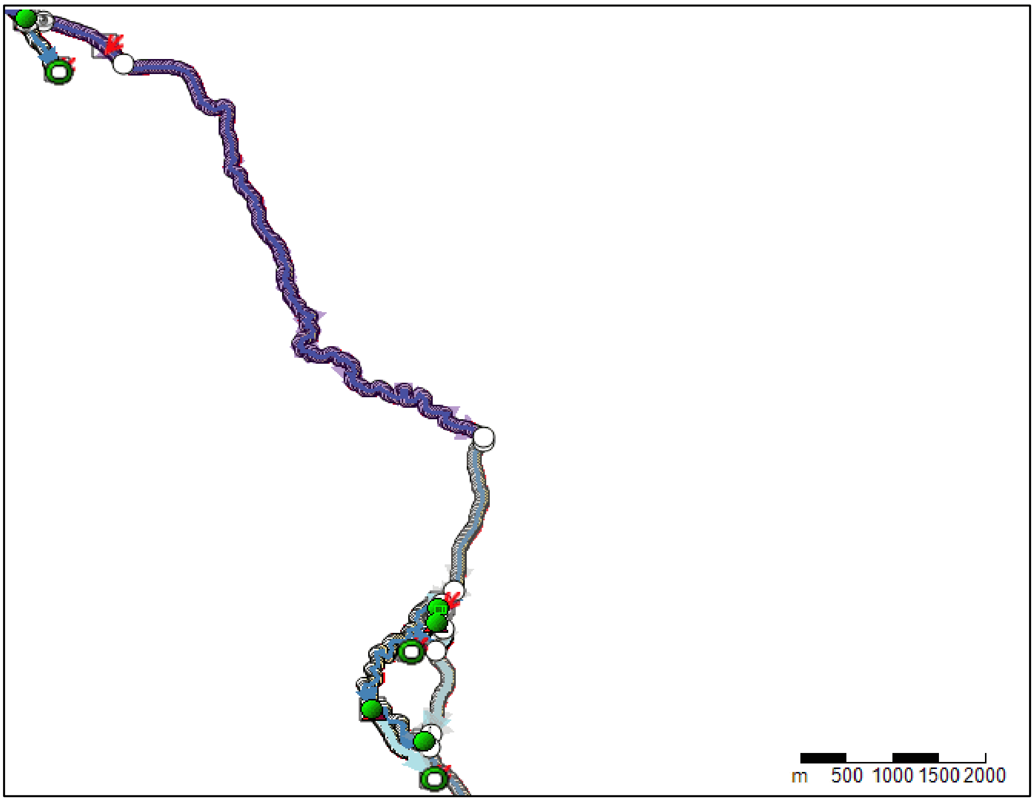

Figure 28 Bandawai thin strip and Bandawai mid sections.

The **Uskof** canal, with its thin strips in both its upper and lower parts use the cross-section shown below in Figure 29, which is an adaptation of the Jerwan aqueduct, to estimate the tributary joining the Khosr (Figure 30).

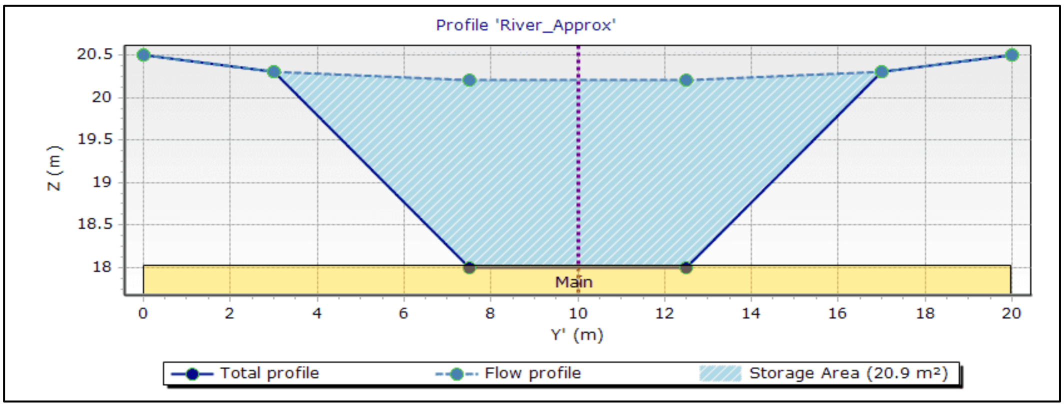

Figure 29 Bandawai River cross-section estimation based on the Jerwan aqueduct.

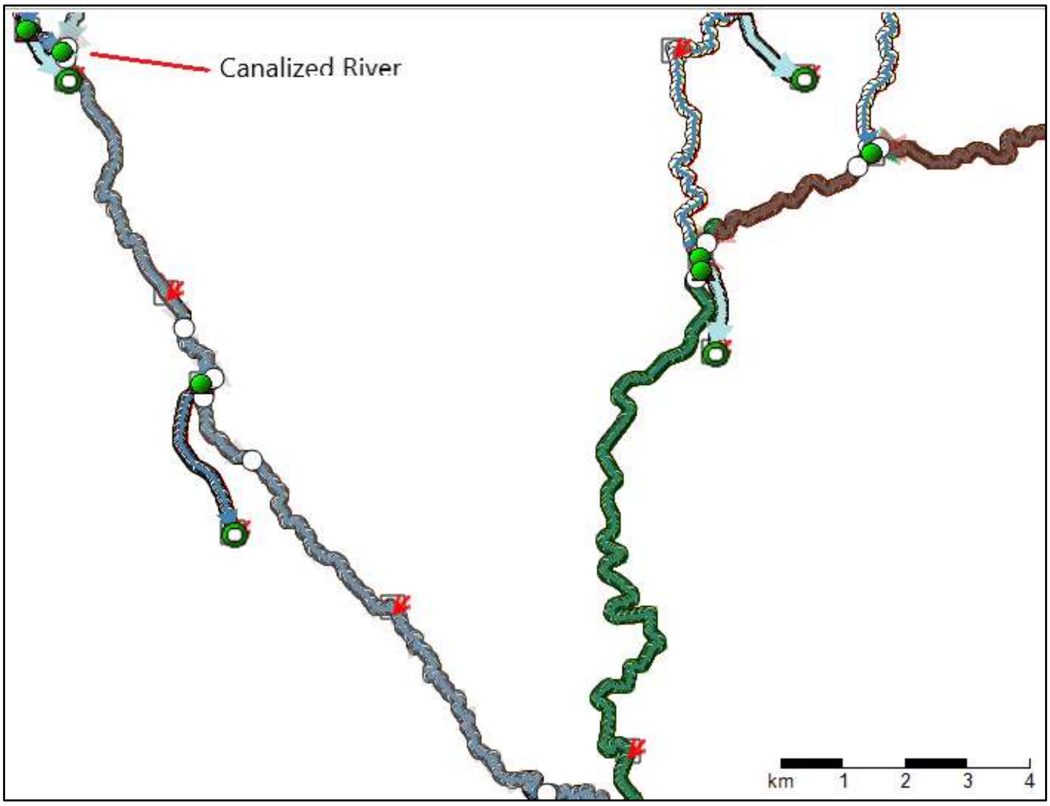

Figure 30 Uskof upper and lower thin strips, where the beginning of the canalized section is shown.

The upper **Khinis** begins with the 133 cross-section featured in Figure 31, with a rock-cut bed roughness. As shown in Figure 33, at the 834 cross-section (Figure 32), the canal has an earthen bed roughness.

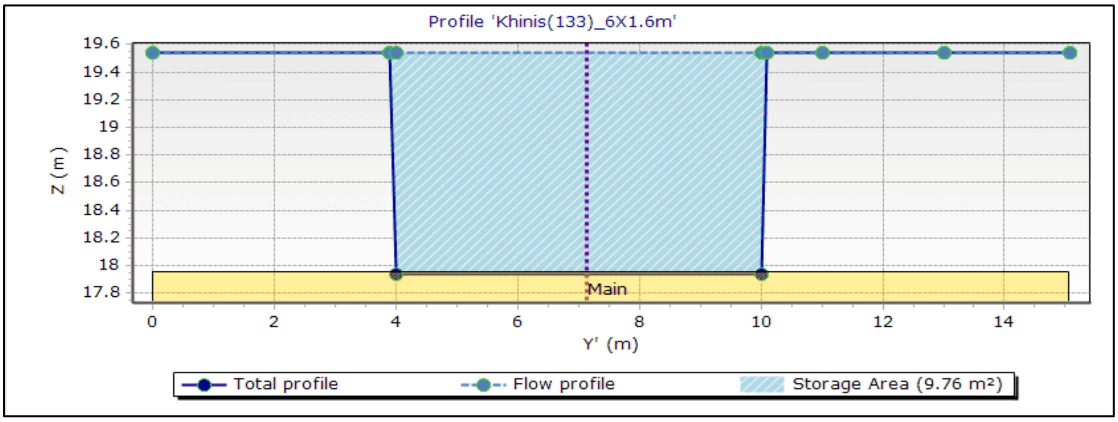

Figure 31 Khinis 133 cross-section adaptation is Sobek.

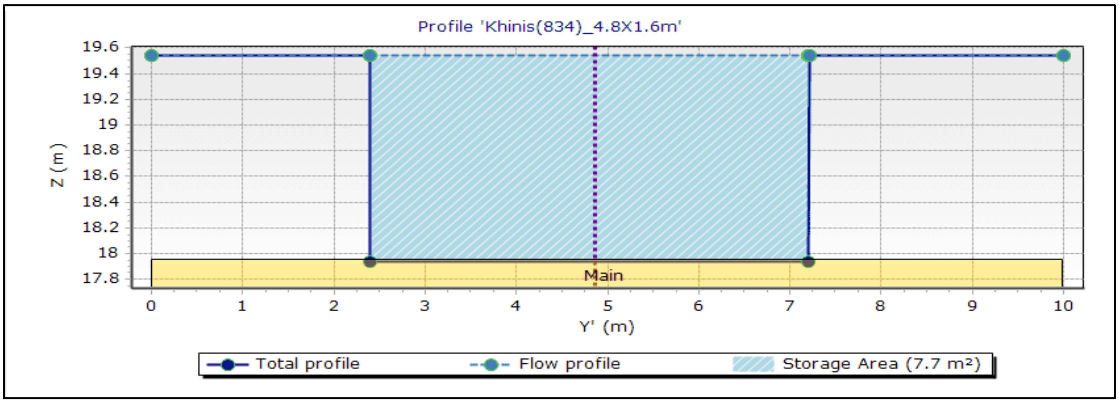

Figure 32 Khinis 834 cross-section adaptation in Sobek.

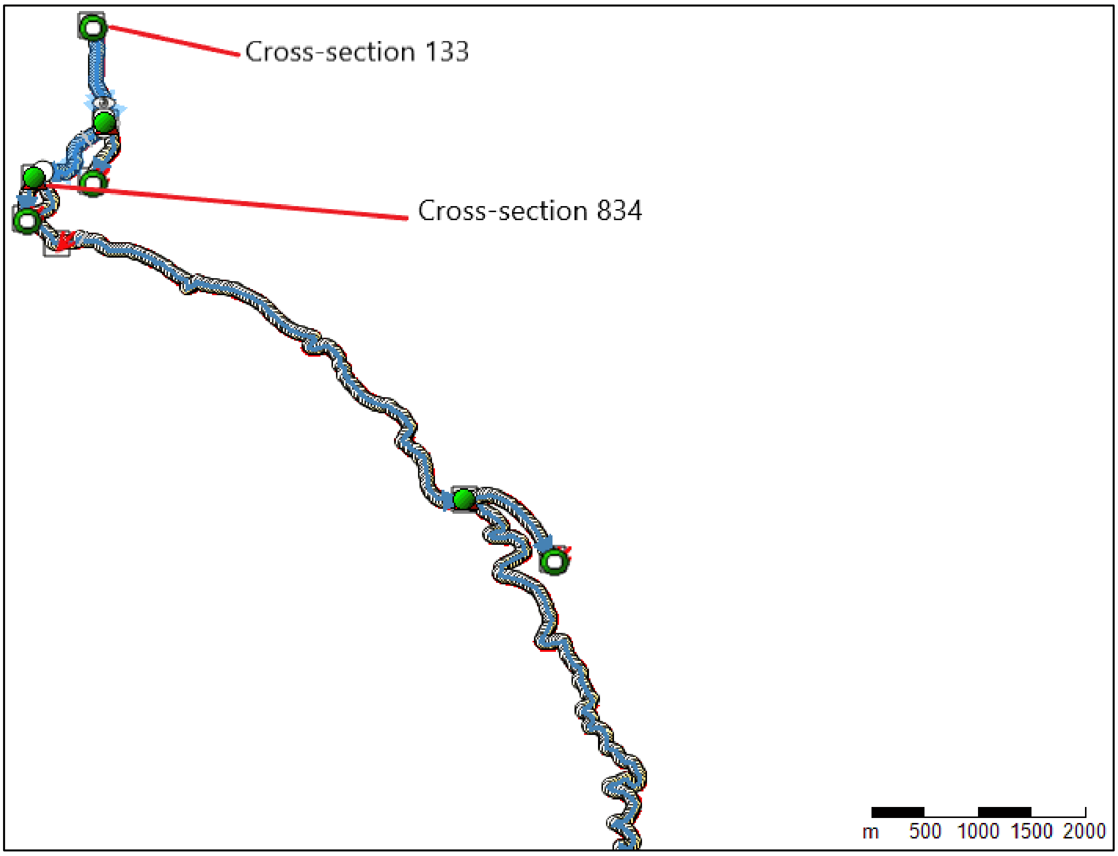

Figure 33 Khinis upper section, marking the start of each cross-section.

Jerwan uses the 834 Khinis earthen cross-section throughout its length, excluding the part defined in Figure 35 as the Jerwan aqueduct. Detailed on this cross-section with a roughness of 0,022 s $m^{1/3}$, are shown in Figure 34.

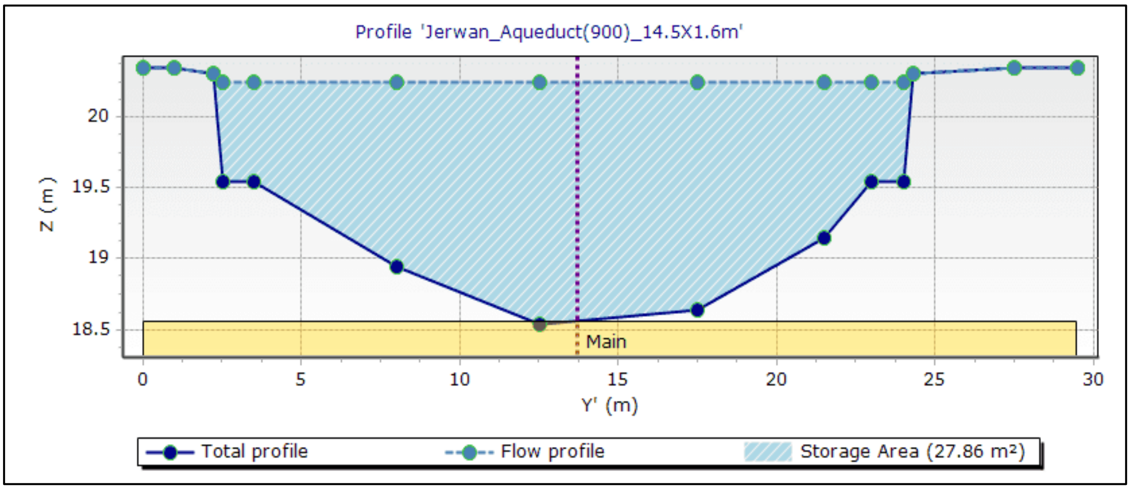

Figure 34 Jerwan aqueduct Sobek adaptation.

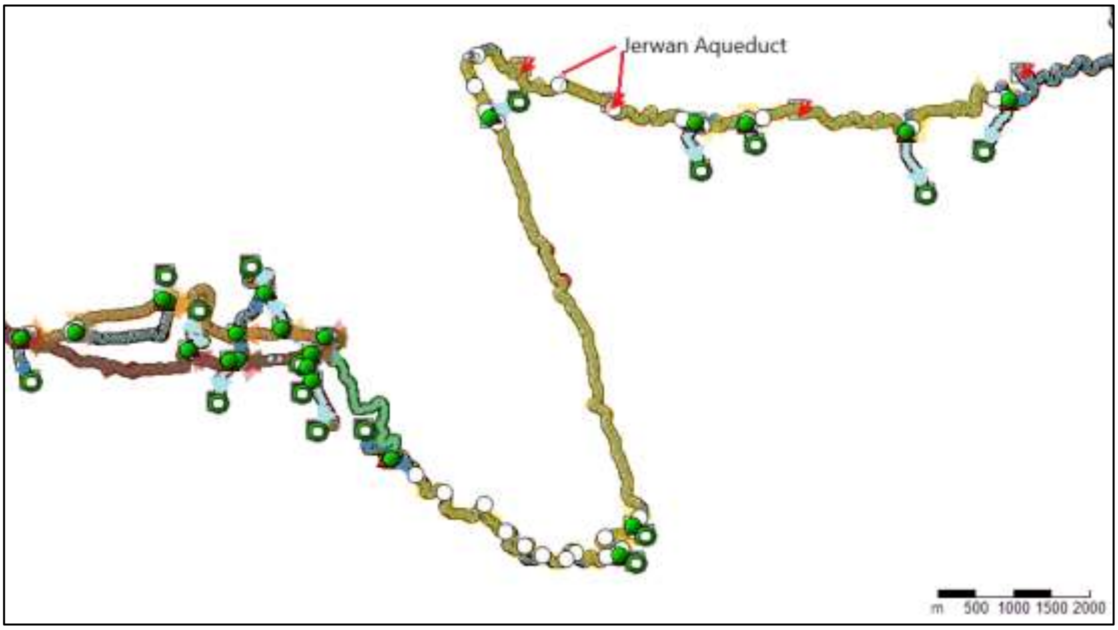

Figure 35 Jerwan area with the aqueduct's extents shown.

The **Badreh** canals are all assumed as earthen, with a cross-section like the 834 Khinis, while the Khosr tributary consists of the same river approximation used for the Uskof sections (Figure 36).

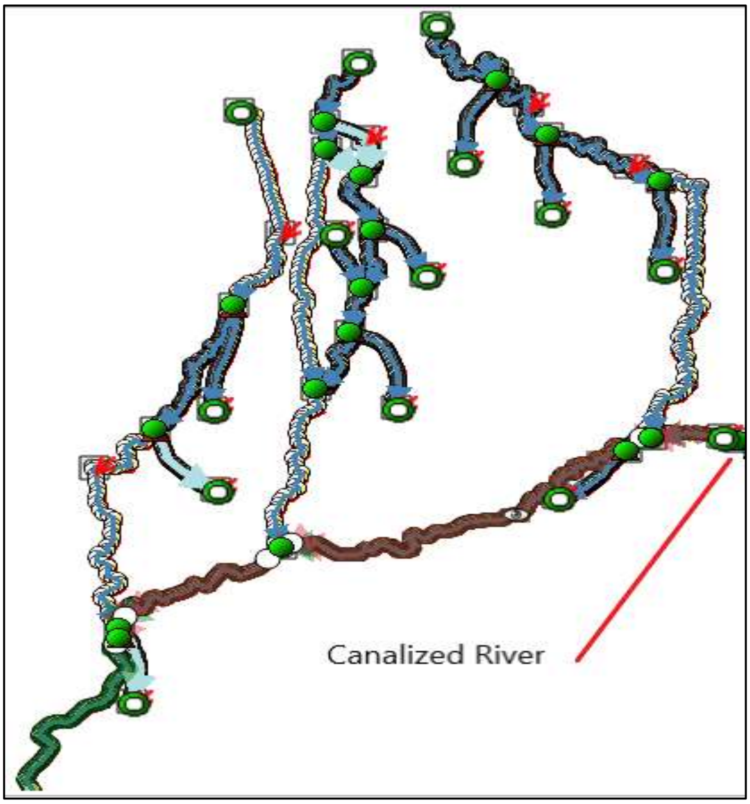

Figure 36 Badreh canals along with Khosr tributary.

For the **Khosr** section the same river approximation as in Khosr tributary and Uskof sections is used, while for the **Kisiri-Nineveh** route, the Khinis 834 cross-section is used (Figure 37).

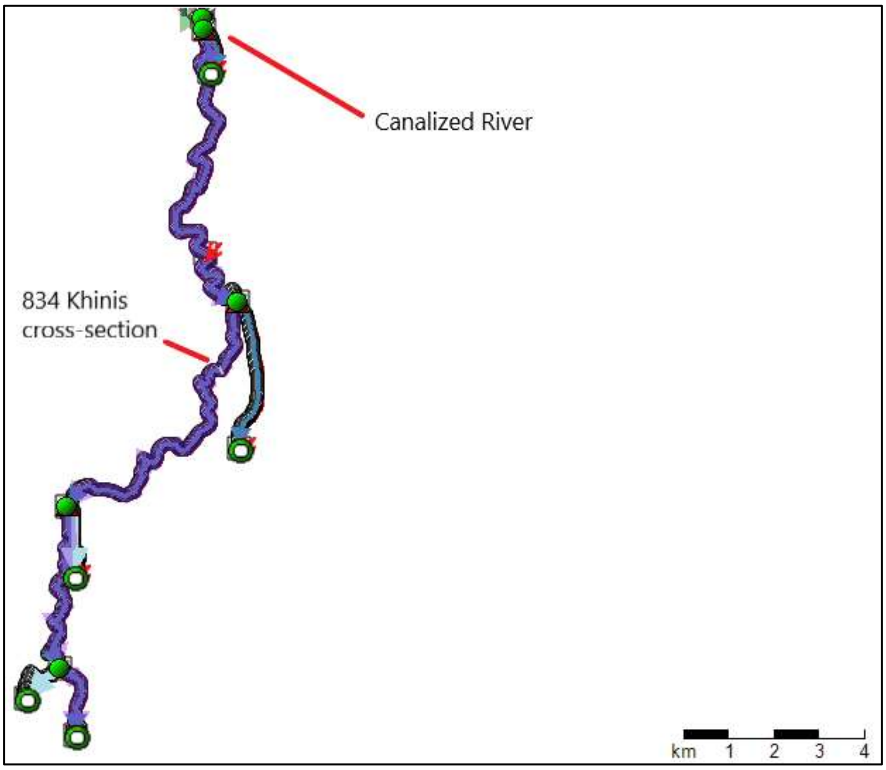

Figure 37 Khosr canalized river and Kisiri earthen route.

Offtakes are modelled as rectangular cross-sections, with two choices for widths (1 or 2 m (both Local and Regional)), and a potential water depth of 1 or 0,5 for Regional and Local systems, respectively. Boundary conditions on offtakes are of the Flow Water level type, with more details shown in the ANNEX in Figure 1, Tables 5, 6 and 7.

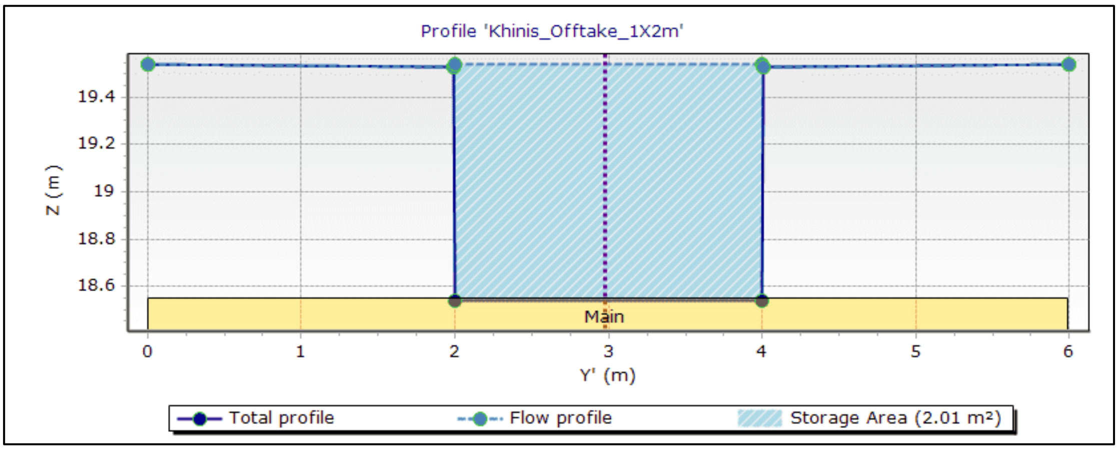

Figure 38 Offtake with a 2 m width and 1 m water depth.

Control Scenarios

Water allocation control is assumed to be achieved using two possible structures: weirs in main reaches and gates on secondary canals. Weirs are placed 20 m after the offtakes on the main canal; their purpose is raising water level, increasing the flow towards the given offtake. Gates are situated around 10 m downstream of the offtake-main reach junction. Manipulating their openings (from open to closed) with a time schedule allows for more flexibility in water flow distribution over upstream-downstream areas within the Regional system.

Three weirs were installed at points where the main canal route splits. These weirs are not related to offtakes. The first location is shown in Figure 28 placed on the left route, while in Figure 35, weirs are positioned at the canal entering the Mumbarak area complex and at its upper (secondary) route second offtake. These secondary routes need weirs as they differ in slopes compared to main section, creating favorable flow conditions for one route if no measures are taken.

Three control scenarios are identified and modelled:

- Maximum Control, utilizing weirs before each offtake and gate manipulation to achieve irrigation needs with lowest water inputs, during calibration.

- Limited Control, assuming weir presence considered possible within a certain distance from the nearest archaeologically identified city or settlement. This distance was arbitrarily set to 5 Km, or around a 2-hour walk, while cities and settlements were provided by the LoNAP team through QGIS files. As in Maximum Control, weirs and gates are set to achieve the required water coverage for fields, with the lowest possible water input during calibration. Figures 38 through 40 show the nearby settlements, while Table 10 indicates weirs and gates used.

- No Control, without weirs in the main reaches and without changing gate openings through the simulation, thus only relying on water inputs to meet water coverage during calibration.

Table 10 Weirs used, and gates manipulated per canal reach, Heavy and Limited Control scenarios for both 1 and 2 m offtake width scenarios. Their sums are provided at the two bottom rows.

	1m				2m			
Control Scenarios	Heavy		Limited		Heavy		Limited	
Canals	Weirs	Gates	Weirs	Gates	Weirs	Gates	Weirs	Gates
Maltai_upper	4	2	3	2	4	2	3	2
Faida	4	0	2	0	4	0	2	0
Bandawai_upper	1	1	1	1	1	1	1	1
Bandawai_up_thin_strip	1	1	0	0	1	1	0	0
Bandawai_mid	1	1	1	1	1	1	1	1
Uskof_upper	1	0	0	0	1	1	0	1
Uskof_lower	1	1	1	1	1	1	1	1
Khinis	3	3	3	3	3	3	3	3
Jerwan	16	6	11	5	16	6	11	5
Koshr_tributary	3	1	2	2	3	2	2	1
Kisiri_Nineveh	1	0	1	0	1	0	1	0
Khosr_thin_strip	2	2	0	1	2	2	0	2
Maltai_low	1	0	1	0	1	0	1	0
Badreh-Jerahiyeh	7	2	5	2	7	2	5	2
Regional	37	18	25	16	37	20	25	17
Local	9	2	6	2	9	2	6	2

Input Scenarios

Water input locations used in Sobek are either in the canal's origin or near a junction with a stream/wadi. The only available data on these locations and junctions are their routes, presented as QGIS images (Figures 39 -42). Sources used are indicated with red circles, while streams are shown in green. Flow amounts used are qualitatively guided by the drainage basins identified through QGIS. These are presented in Figure 42, with numbers in their center representing the basin's area in hectares.

Table 11 presents the canals with their associated drainage basin hectares. These drainage basins allow setting (as no other data on water inputs are available) flow amounts injected in the system. Inflow amounts are guided by the sum of demands presented in Table 9 for Regional and Local systems, as well as potential inflows (m3/s) in Table 11. The latter are calculated using an arbitrary runoff coefficient of 65%, mean annual precipitation (mm) for each location (Nineveh=278, Navkur=340, Faida=325) creating mean annual inflow, cool season (90% of rainfall in 6 months Nov-Apr) inflow and Dry, Wet alternatives. Dry and Wet estimates are based on the region's max/min variability between 1979-2010, presenting 64% decrease and around 77% increase in 1999 and 1980, respectively. Worth mentioning is that basins draining in Faida, Maltai, Khinis, Jerwan and Ba'dreh canals most likely experience higher annual rainfall amounts (situated in the Zagros mountains) and therefore higher potential discharges (Sinha et al., 2019). More details on inflows chosen are found in Table 12, 13 and the Calibration-Model Runs section below.

Table 11 Canal with associated drainage basin area in hectares, required delivery flow, estimated annual mean, cool season flow, as well as Min and Max cool season inflow.

Canals connected with inflows	**Drainage Basins (ha)**	**Delivery flow required**	**Annual mean flow**	**Cool season inflow**	**Min cool season inflow**	**Max cool season inflow**
Maltai	15691.964	0.95775463	1.05115658	1.897279874	0.8727487	3.358185
Faida	426.909	0.684606481	0.02859733	0.051616602	0.0237436	0.091361
Bandawai upper Wadi	9202.766	0.192958333	0.64491733	1.164040342	0.5354586	2.060351
Bandawai-Uskof	10690.323	0.80625	0.7491633	1.352198594	0.6220114	2.393392
Khinis	51167.03	0.38125	3.58571589	6.472020164	2.9771293	11.45548
Ba'dreh	17600.565	3.479861111	1.23342366	2.226261942	1.0240805	3.940484
Jerwan	5310.868	7.243055556	0.37217841	0.671761577	0.3090103	1.189018
Koshr-tributary	7988.07	0.46875	0.55979308	1.010395759	0.464782	1.7884
Kisiri-Koshr	5776.473	4.84375	0.33098956	0.597417967	0.2748123	1.05743

Two input scenarios are assumed for each control scenario, representing a **Reference** year with water requirements met and a **Dry** year, representing low flow years. An extra setting is created for the scenario without control, since meeting its needs requires larger water inputs compared to other scenarios. The No Control scenario therefore also includes a **Wet** year.

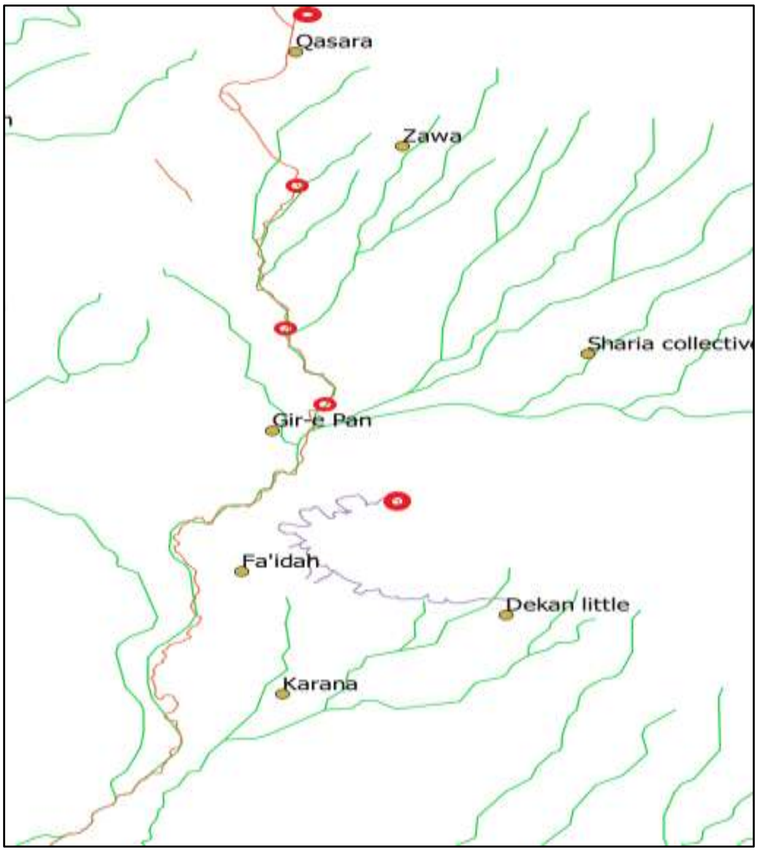

Figure 39 Local system, Maltai and Faida’s input locations are shown in red while streams/wadis in green, along with archeologically identified settlements.

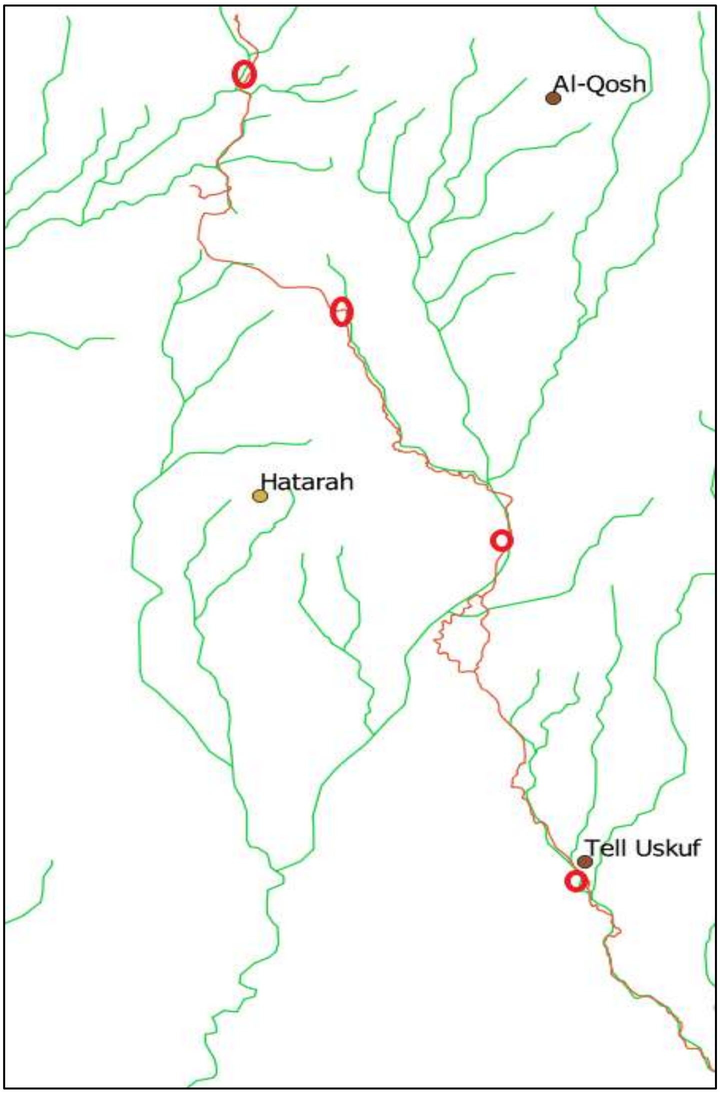

Figure 40 Bandawai-Uskof canals, nearby settlements, streams crossing them (green) and input locations (red).

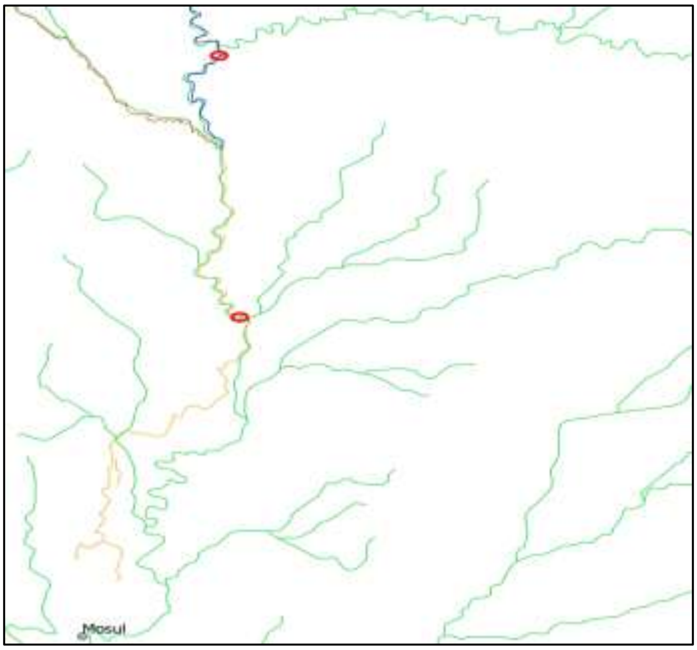

Figure 41 Khosr and Kisiri reaches with nearby settlements, streams crossing them (green) and input locations (red).

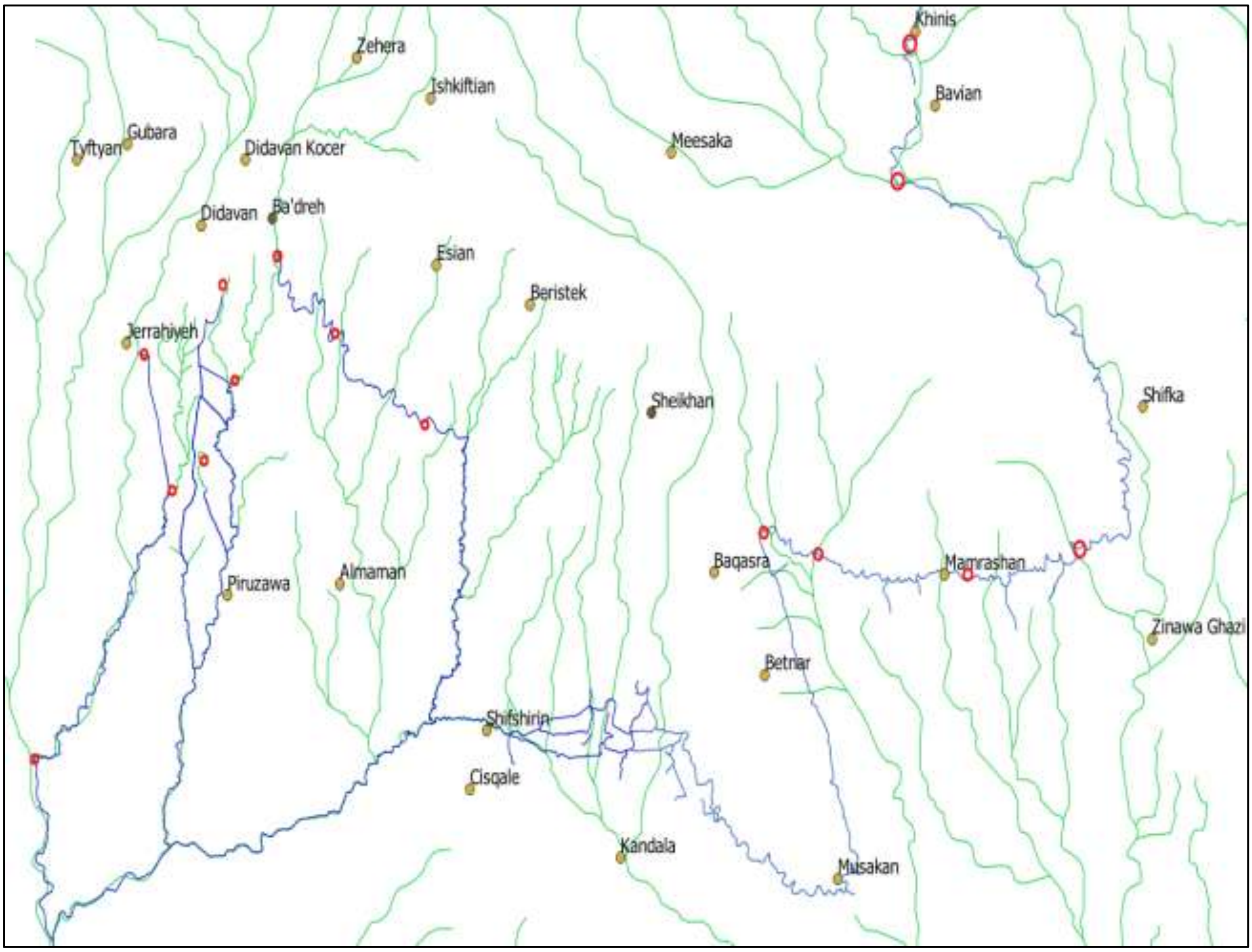

Figure 42 Khinis, Jerwan, Badreh and Khosr tributary reaches with nearby settlements, streams crossing them (green) and input locations (red).

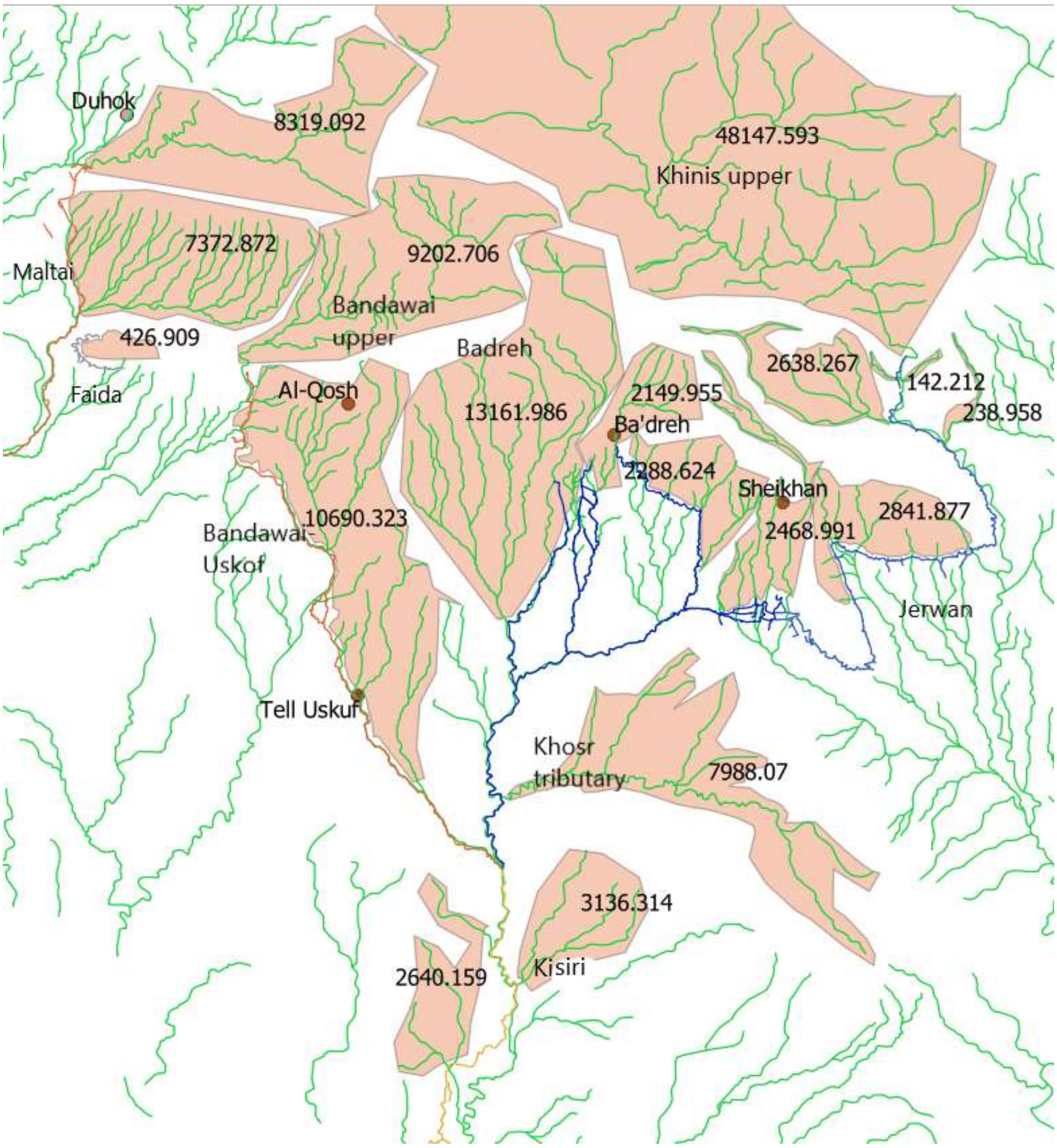

Figure 43 Drainage basins associated with canals (pink) and their area in hectares, along with rivers, streams/wadis (green) and bigger settlements in the area.

Calibration-Model Runs

Initially, the Maximum Control scenario with inputs equal to the sum of the water requirements for all areas per system (see Table 9) and arbitrary weir crest levels is run. The calibration check to satisfy water coverage over the selected areas is done through manipulation of weir crest levels and gate opening time schedules. When these settings no longer significantly affect the resulting coverage, specific water inputs are increased to meet coverage needs. The same process is carried out for the Limited Control and No Control scenarios.

For the first two control scenarios, the calibration year input is considered as a Reference scenario while a Dry year is modeled with the former's inputs halved.

In the absence of control, calibration takes place on the Wet year, while the Reference and Dry years are produced by taking half and a quarter of the inputs, respectively. Tables 12 and 13 present inputs per area in m^3/s for Maximum and Limited Control scenarios, for Wet, Reference and Dry years and for 1 and 2 m offtake widths, respectively.

Table 12 1 m Offtake width input flows m3/s per area, Control, and Input scenarios.

Control		**Absent**		**Heavy**		**Limited**	
Canals	Input flow Wet year	Refrence Inputs	Input flow Dry year	Input flow	Input flow Dry year	Input flow	Input flow Dry year
Maltai_upper	2.65	1.325	0.6625	1.2	0.6	1.2	0.6
Faida	2	1	0.5	1	0.5	1	0.5
Bandawai_upper	6.6	3.3	1.65	0.55	0.275	3.3	1.65
Bandawai_up_thin_strip	0.7	0.35	0.175	0.35	0.175	0.35	0.175
Bandawai_mid	5	2.5	1.25	0.9	0.45	0.9	0.45
Uskof_upper	0.2	0.1	0.05	0.1	0.05	0.1	0.05
Uskof_lower	0.2	0.1	0.05	0.1	0.05	0.1	0.05
Khinis	10.2	5.1	2.55	5.1	2.55	5.1	2.55
Jerwan	10	5	2.5	5	2.5	5	2.5
Koshr_tributary	0.6	0.3	0.15	0.3	0.15	0.3	0.15
Kisiri_Nineveh	0	0	0	0	0	0	0
Khosr_thin_strip	0.4	0.2	0.1	0.2	0.1	0.2	0.1
Maltai_low	0.8	0.4	0.2	0.4	0.2	0.4	0.2
Badreh-Jerahiyeh	10.11	5.055	2.5275	5.45	2.725	5.405	2.7025
Regional	44.01	22.005	11.0025	18.05	9.025	20.755	10.3775
Local	5.45	2.725	1.3625	2.6	1.3	2.6	1.3

Table 13 2 m Offtake width input flows m3/s per area, Control and Input scenario.

Control		**Absent**		**Heavy**		**Limited**	
Canals	Input flow Wet year	Refrence Inputs	Input flow Dry year	Input flow	Input flow Dry year	Input flow	Input flow Dry year
Maltai_upper	2.4	1.2	0.6	1.2	0.6	1.2	0.6
Faida	2.1	1.05	0.525	1.05	0.525	1.05	0.525
Bandawai_upper	5.6	2.8	1.4	0.55	0.275	2.8	1.4
Bandawai_up_thin_strip	0.7	0.35	0.175	0.35	0.175	0.35	0.175
Bandawai_mid	3.7	1.85	0.925	0.9	0.45	0.9	0.45
Uskof_upper	0.2	0.1	0.05	0.1	0.05	0.1	0.05
Uskof_lower	0.2	0.1	0.05	0.1	0.05	0.1	0.05
Khinis	10.2	5.1	2.55	5.1	2.55	5.1	2.55
Jerwan	10	5	2.5	5	2.5	5	2.5
Koshr_tributary	0.6	0.3	0.15	0.3	0.15	0.3	0.15
Kisiri_Nineveh	0	0	0	0	0	0	0
Khosr_thin_strip	0.4	0.2	0.1	0.2	0.1	0.2	0.1
Maltai_low	0.8	0.4	0.2	0.4	0.2	0.4	0.2
Badreh-Jerahiyeh	10.9	5.45	2.725	5.45	2.725	5.45	2.725
Regional	41.9	20.95	10.475	17.75	8.875	20	10
Local	5.3	2.65	1.325	2.65	1.325	2.65	1.325

References

Arcement, G. J., & Schneider, V. R. (1989). Guide for selecting Manning's roughness coefficients for natural channels and flood plains. US Geological Survey Water-Supply Paper*, 2339. https://doi.org/10.3133/wsp2339*

Buringh, R. P. (1960). SOILS AND SOIL CONDITIONS IN IRAQ.

Deltares. (2019a). Sobek 3.7 D-Flow 1D User Manual.

Deltares. (2019b). Sobek 3.7 D-RTC User Manual.

Dr. Xing Fang, Department of Civil Engineering, L. U. (2000). Open Channel Flow Calculator. *Retrieved from https://www.eng.auburn.edu/~xzf0001/Handbook/Channels.html*

Morandi Bonacossi, D. (2018). THE CREATION OF THE ASSYRIAN HEARTLAND: NEW DATA FROM THE 'LAND BEHIND NINEVEH.'

Morandi Bonacossi, D. (2019). Water for Nineveh. Water for Assyria*, 1–6.*

https://doi.org/10.2307/j.ctvcm4fg3.4

Reculeau, H. (2011). Climate, Enviroment and Agriculture in Assyria in the 2nd Half of the 2nd Millennium BCE *(Studia Cha; H. Kuhne, Ed.). Harrassowitz.*

Reculeau, H. (2018). On Some Metrological Issues Affecting Yield Estimates in Second-Millennium BCE Upper Mesopotamia. Journal of Cuneiform Studies*,* 70*(1), 87–114. https://doi.org/10.5615/jcunestud.70.2018.0087*

Sinha, A., Kathayat, G., Weiss, H., Li, H., Cheng, H., Reuter, J., … Lawrence Edwards, R. (2019). Role of climate in the rise and fall of the neo-assyrian empire. Science Advances*,* 5*(11), 1–11. https://doi.org/10.1126/sciadv.aax6656*

Ur, J. (2005). Sennacherib's northern Assyrian canals: New insights from satellite imagery and aerial photography. Iraq*, Vol. 67, pp. 317–345. https://doi.org/10.1017/s0021088900001418*